AD-A077 375 ALABAMA UNIV IN HUNTSVILLE DEPT OF MECHANICAL ENGINEERING F/G 20/4
FINITE ELEMENT ANALYSIS OF SUBSONIC TRANSONIC, AND SUPERSONIC F--ETC(U)
OCT 79 T J CHUNG DAAG29-76-G-0033
UNCLASSIFIED UAH-RR-228 ARO-13098.3-E NL

1 OF 1
AD
A077375

END
DATE
FILMED
1-80
DDC

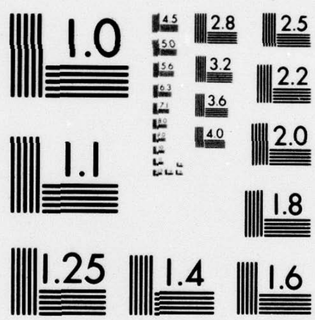

MICROCOPY RESOLUTION TEST CHART
NATIONAL BUREAU OF STANDARDS-1963-A

UAH Research Report No. 228

FINITE ELEMENT ANALYSIS OF SUBSONIC, TRANSONIC, AND SUPERSONIC FLOWS AROUND MISSILES

Final Report

T. J. Chung

October, 1979

U.S. Army Research Office

[redacted]

The University of Alabama in Huntsville
Huntsville, Alabama

Approved for Public Release
Distribution Unlimited

UAH Research Report No. 228

FINITE ELEMENT ANALYSIS OF SUBSONIC, TRANSONIC, AND SUPERSONIC FLOWS AROUND MISSILES

Final Report

T. J. Chung

October, 1979

U.S. Army Research Office

DAAG-76-G-0033

The University of Alabama in Huntsville
Huntsville, Alabama

DISCLAIMER

THE FINDINGS OF THIS REPORT ARE NOT TO BE CONSTRUED AS AN OFFICIAL DEPARTMENT OF THE ARMY POSITION UNLESS SO DESIGNATED BY OTHER AUTHORIZED DOCUMENTS.

14 UAH-RR-228

SECURITY CLASSIFICATION OF THIS PAGE (When Data Entered)

REPORT DOCUMENTATION PAGE		READ INSTRUCTIONS BEFORE COMPLETING FORM
1. REPORT NUMBER	2. GOVT ACCESSION NO.	3. RECIPIENT'S CATALOG NUMBER
4. TITLE (and Subtitle) 6 Finite Element Analysis of Subsonic Transonic, and Supersonic Flows Around Missiles.		5. TYPE OF REPORT & PERIOD COVERED 9 Final Report, 1976-1979.
		6. PERFORMING ORG. REPORT NUMBER
7. AUTHOR(s) 10 T. J. Chung		8. CONTRACT OR GRANT NUMBER(s) 15 DAAG29-76-G-0033
9. PERFORMING ORGANIZATION NAME AND ADDRESS The University of Alabama in Huntsville Huntsville, Ala. 35807		10. PROGRAM ELEMENT, PROJECT, TASK AREA & WORK UNIT NUMBERS Dept. of Mechanical Engrg.
11. CONTROLLING OFFICE NAME AND ADDRESS U. S. Army Research Office Post Office Box 12211 Research Triangle Park, NC 27709		12. ~~REPORT DATE~~ 11 ~~October,~~ Oct 1979
		13. NUMBER OF PAGES 12 72
14. MONITORING AGENCY NAME & ADDRESS(if different from Controlling Office) The U.S. Army Research Office Research Triangle Park, NC 27709 18 ARO 19 13098.3-E		15. SECURITY CLASS. (of this report) Unclassified
		15a. DECLASSIFICATION/DOWNGRADING SCHEDULE NA

16. DISTRIBUTION STATEMENT (of this Report)

Approved for public release; distribution unlimited.

17. DISTRIBUTION STATEMENT (of the abstract entered in Block 20, if different from Report)

NA

18. SUPPLEMENTARY NOTES

The findings in this report are not to be construed as an official Department of the Army position, unless so designated by other authorized documents.

19. KEY WORDS (Continue on reverse side if necessary and identify by block number)

Aerodynamics, Missiles, Finite Elements, Transonic Flow

This report examines

20. ABSTRACT (Continue on reverse side if necessary and identify by block number)

The work carried out herein represents the Galerkin finite element method for solving aerodynamics problems with emphasis on transonic flows. A shock element concept was proposed and computations ~~have been~~ were carried out. In this process, a quadratic isoparametric element is divided into quadrants with each quadrant having independent trial functions. This idea allows discontinuities at the center of an element and shocks are allowed to develop freely. Rankin-Hugoniot conditions are satisfied accurately. 409 768 (over)

DD FORM 1 JAN 73 1473 EDITION OF 1 NOV 65 IS OBSOLETE

Unclassified JOB

SECURITY CLASSIFICATION OF THIS PAGE (When Data Entered)

cont

the reporting

20.

Although this method is efficient until freestream Mach number reaches approximately 0.95, the solution seems to deteriorate significantly for M > 0.95. Toward the end of ~~this contract research~~ period, the author proposed a new approach -- optimal control penalty finite elements. This method is suited ideally for problems of discontinuity and shock waves as a consequence of changes in the type of partial differential equations. The resulting equations are ~~sym-~~ sym metric and positive-definite, their solution being type-independent. Numerous examples indicate that both stability and accuracy are maintained very satisfactorily for Tricomi and small perturbation equations. Detailed calculations applied to the full potential equations using this approach are beyond the scope of the present study.

Accession For	
NTIS GRA&I	
DDC TAB	
Unannounced	
Justification______	
By______	
Distribution/	
Availability Codes	
Dist	Avail and/or special
A	

TABLE OF CONTENTS

ACKNOWLEDGMENT

This research has been supported by the U.S. Army Research Office, Research Triangle Park, North Carolina. Dr. Robert Singleton was the technical monitor.

Graduate students at the Mechanical Engineering Department of the University of Alabama in Huntsville assisted in various phases of this research. In particular, I would like to thank C. G. Hooks and D. W. Miller for their contributions in developing computer programs.

1. INTRODUCTION

With the finite element method recognized as an efficient tool in solving engineering problems in solid mechanics during the 1960's the applied mathematician began to explore the finite element theory in search for mathematical foundations. It was not until the late 1960's or the early 1970's that the finite element theory was rediscovered as a part of the classical approximation theory, functional analysis, and Sobolev space theory, [1-5]. In recent years, finite element applications into fluid mechanics, heat transfer, electromagnetic field, and other areas have been increasingly active [6,7] as the concept of the finite element theory has reached a considerable degree of maturity at least in linear problems.

In fluid mechanics applications, computational difficulties arise from nonlinearity associated with convective terms in Navier-Stokes equation and energy equation. Complications occur also in the potential equation governing high Mach number flows. The standard Galerkin procedure is found adequate for low Mach numbers, low Reynold numbers, low Peclet numbers. However, the solution stability and rates of convergence in the Galerkin formulation deteriorate significantly for high speed flows [7,8]. Refinements of mesh would improve the solution [7,8] but are quite costly. A recent development in an effort to remedy unstable solutions in high speed flows is "upwind finite elements" [9-12]. Unfortunately, however, upwinding leads to undesirable damping and accuracy is not guaranteed [13,14]. To overcome these deficiencies, more recently, the optimal control least squares finite elements

have been employed with all second order derivatives reduced to the first order resulting in a symmetric positive-definite system of equations [15,16, 17]. The penalty method is utilized in handling all constraint equations in which properly adjusted penalty constants play a major role in acquiring convergence, stability, and accuracy.

The main part of the present report consists of formulations of Galerkin finite element equations applied in aerodynamics with emphasis on transonic flows. In particular, we develop a shock element with continuous and discontinuous trial functions. Rankin-Hugoniot conditions are adequately satisfied for shock elements. Examples are shown for free stream Mach numbers up to 0.95. Deterioration of solution begins to appear for $M > 0.95$.

Toward the end of the contract period, the author proposed a new approach, called the optimal control penalty finite elements, in order to overcome instability in solution. Details of this new theory are presented and numerous example problems are given to demonstrate its validity and potentiality. These examples are compared with exact solutions in Tricomi and small perturbation equations. Detailed calculations in the full potential equation using this new theory are beyond the scope of the present study.

2. PRELIMINARIES - TRANSONICS

The main difficulties in the study of transonic flows stem from the nonlinearity of the governing equations, existence of shocks, and the possibility of nonphysical solutions (entropy condition violated). These problems arise in finite difference techniques particularly with complicated geometries. The objective of the present study is to introduce the finite element analysis in an effort to overcome these difficulties.

We consider an inviscid, compressible fluid and assume that the flow is potential such that

$$\underset{\sim}{\nabla} \cdot \rho \underset{\sim}{V} = 0 \qquad \text{in } \Omega \tag{2.1}$$

$$\rho = \rho_0 \left(1 - \frac{|\underset{\sim}{V}|^2}{\frac{\gamma+1}{\gamma-1} C_*^2}\right)^{\frac{1}{\gamma-1}} \tag{2.2}$$

$$\underset{\sim}{V} = \underset{\sim}{\nabla}\phi \tag{2.3}$$

where ϕ is the velocity potential, ρ is the density of the fluid, γ is the ratio of specific heats, and C_* is the critical velocity.

It is possible to rewrite (2.2) in the form

$$\rho = \left(1 - K\ |\underset{\sim}{\nabla}\phi|^2\right)^{\alpha} \rho_0 \tag{2.4}$$

where $\rho_0 = 1$, $K = \frac{\gamma-1}{\gamma+1}\ \frac{1}{C_*^2}$, and $\alpha = \frac{1}{\gamma-1}$.

As shown in Fig. 2.1, the flow is assumed to be uniform on Γ_∞ and tangential at Γ_B, implying that

$$\frac{\partial\phi}{\partial n} = \underset{\sim}{V} \cdot \underset{\sim}{n} \qquad \text{on} \quad \Gamma_\infty \tag{2.5}$$

$$\frac{\partial\phi}{\partial n} = 0 \qquad \text{on} \quad \Gamma_B \tag{2.6}$$

In two-dimensional problems, the boundary condition for the trailing edge may be chosen as

$$\phi = 0 \qquad \text{at TE} \tag{2.7}$$

It should also be noted that ϕ is discontinuous across the cutting-line. The lift L is defined as

$$\phi^+ - \phi^- = L \tag{2.8}$$

Here we must use the Kutta-Joukowsky condition to find the lift such that

$$P^+ = P^- \qquad \text{at TE} \tag{2.9}$$

In case of a shock the Rankine-Hugoniot conditions must be satisfied such that

$$[\![\rho \underset{\sim}{V} \cdot \underset{\sim}{n}]\!]^+ = [\![\rho \underset{\sim}{V} \cdot \underset{\sim}{n}]\!]^- \tag{2.10}$$

and the tangential component of the velocity is continuous.

Consider a disk shown in Figs. 2.2 and 2.3 . Here the Kutta-Joukowsky condition is automatically satisfied due to symmetry. There are two possible velocity distributions as represented by Figs. 2.3 and 2.4 .An expansion shock prevails in Fig. 2.2 in violation of thermodynamics laws whereas Fig. 2.3 is physically consistent. It is necessary to impose the entropy condition to prevent expansion shocks. It is well known that in finite difference methods the entropy condition is represented by an upwind scheme or artificial viscosities in the supersonic region. In the finite element method, however, the Lagrange multipliers are utilized to impose the entropy condition. The details will be shown in the following section.

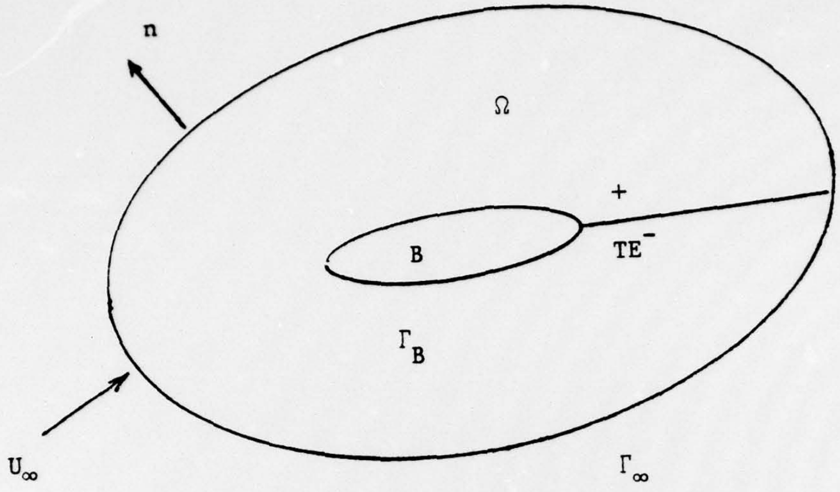

Figure 2.1 Boundary conditions of airfoil

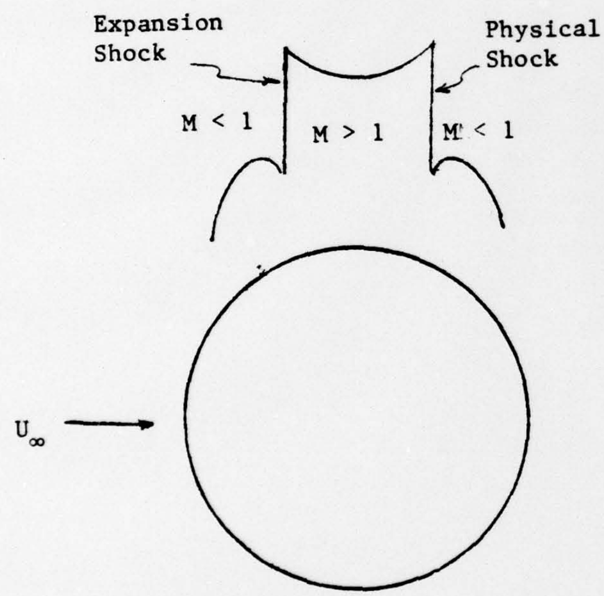

Figure 2.2 Expansion Shock

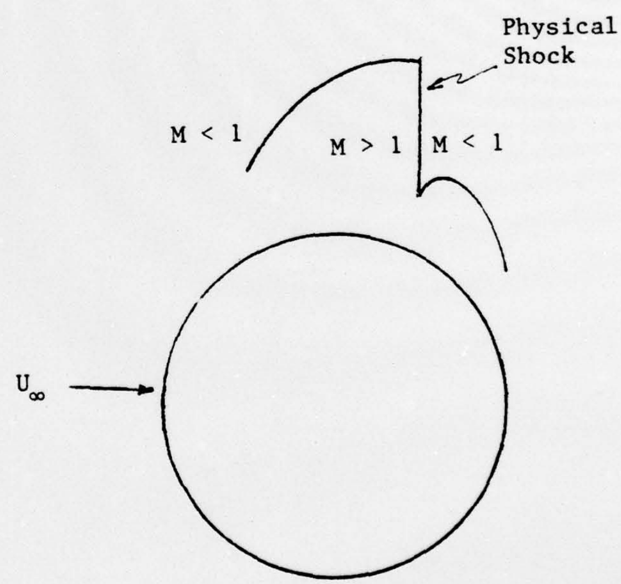

Figure 2.3 Physical Shock

3. GALERKIN AND VARIATIONAL METHODS

3.1 Galerkin Approach

When viscosity is negligible in compressible fluids, the analysis becomes simplified. Physically, we may consider the fluid to be a perfect gas, particularly in aerodynamics design. In this context, we begin with Euler and continuity equations of the form

$$V_{i,j}V_j + \frac{1}{\rho} P_{,i} = 0 \tag{3.1}$$

$$(\rho V_i)_{,i} + \frac{e\rho V_2}{x_2} = 0 \tag{3.2}$$

where e = 0 and e = 1 for two-dimensional flow and axially symmetric flow, respectively.

The total enthalpy $\hat{H}$ and entropy η are constant along each streamline. Therefore, we must have

$$d\hat{H} = \hat{H}_{,i}V_i dt = 0$$

or

$$\hat{H}_{,i}V_i = 0 \tag{3.3}$$

and

$$d\eta = \eta_{,i}V_i dt = 0$$

or

$$\eta_{,i}V_i = 0 \tag{3.4}$$

Here it should be noted that (3.4) is valid everywhere except for passage through a shock wave. Along the streamline, the velocity of sound is

$$a = \left(\sqrt{\frac{\partial P}{\partial \rho}}\right)_{\eta=\text{const}} = \sqrt{\frac{\gamma P}{\rho}} = \sqrt{\gamma RT} \tag{3.5}$$

The relation between pressure and density in an ideal gas with c_p and c_v constant is given by

$$\frac{P}{\rho^\gamma} = \frac{P_0}{\rho_0^\gamma} \exp\left(\frac{\eta - \eta_0}{c_v}\right) = C \exp\left(\frac{\eta}{c_v}\right) \tag{3.6}$$

where P_0, ρ_0, and η_0 are the initial conditions and $\gamma = c_p/c_v$, and the function C remains constant along each streamline. In view of (3.5) and (3.2), we obtain

$$P_{,i} = a^2\rho_{,i} - \frac{\rho a^2}{c_p}\eta_{,i} - \frac{\rho a^2}{\gamma} \quad (\ell nC)_{,i} \tag{3.7}$$

Rewriting (3.1) in the form

$$\frac{1}{2}(V_jV_j)_{,i} - \varepsilon_{ijk}\varepsilon_{kmn}V_jV_{n,m} + \frac{1}{\rho}P_{,i} = 0 \tag{3.8}$$

and from the definitions of enthalpy and entropy,

$$H = c_pT = \frac{\gamma}{\gamma - 1}\;\frac{P}{\rho} \tag{3.9}$$

$$\eta = c_v \ell n \frac{P}{\rho^\gamma} \tag{3.10}$$

we obtain

$$T\eta_{,i} + \varepsilon_{ijk}\varepsilon_{kmn}V_jV_{n,m} - (H + \frac{1}{2}V_jV_j)_{,i} = 0 \tag{3.11}$$

For the direction normal to the streamline, (3.11) becomes

$$T\frac{\partial\eta}{\partial n} - \frac{\partial\hat{H}}{\partial n} + \varepsilon_{ijk}\varepsilon_{kmn}V_jV_{n,m}n_i = 0$$

where

$$\hat{H} = H + \frac{1}{2}V_jV_j \tag{3.12}$$

For two-dimensional or axially symmetric flow,

$$\varepsilon_{ijk}\varepsilon_{kmn}V_jV_{n,m}n_i = -\overset{*}{V}(V_{2,1} - V_{1,2}) \tag{3.13}$$

where

$$\overset{*}{V} = V_2n_1 - V_1n_2 \tag{3.14}$$

Hence,

$$V_{2,1} - V_{1,2} = -\frac{1}{\overset{*}{V}}\left(\frac{\partial\hat{H}}{\partial n} - \frac{a^2}{\gamma R}\frac{\partial\eta}{\partial n}\right) \tag{3.15}$$

Multiplying (3.1) by V_i and substituting (3.5) and (3.2) into (3.1) yields

$$V_iV_jV_{i,j} + \frac{a^2}{\rho}V_i\rho_{,i} = 0$$

$$V_iV_jV_{i,j} - a^2\left(V_{k,k} + \frac{eV_2}{x_2}\right) = 0 \tag{3.16}$$

Expanding (3.16) gives

$$\left[1 - \left(\frac{V_1}{a}\right)^2\right]V_{1,1} + \left[1 - \left(\frac{V_2}{a}\right)^2\right]V_{2,2} - \frac{V_1V_2}{a^2}\left(V_{1,2} + V_{2,1}\right) + \frac{eV_2}{x_2} = 0 \tag{3.17}$$

Adding and subtracting $\frac{V_1V_2}{a^2}V_{1,2}$ in (3.17) and substituting from (3.15) yield

$$\left[1 - \left(\frac{V_1}{a}\right)^2\right]V_{1,1} + \left[1 - \left(\frac{V_2}{a}\right)^2\right]V_{2,2} - \frac{2V_1V_2}{a^2}V_{1,2} + \frac{eV_2}{x_2} = E \tag{3.18}$$

in which

$$E = \frac{V_1V_2}{\overset{*}{V}}\left(\frac{1}{\gamma R}\frac{\partial\eta}{\partial n} - \frac{1}{a^2}\frac{\partial\hat{H}}{\partial n}\right) \tag{3.19}$$

This is the most general form of the governing equation for two-dimensional or axially symmetric inviscid compressible flows for subsonic, transonic, and supersonic speeds.

The solution of (3.18) for a two-dimensional case may be obtained by the method of characteristics by transforming into hodograph plane. This is not possible, however, for axially symmetric flow due to the presence

of the term eV_2/x_2. If the entropy η and enthalpy H are constants in the direction normal to the surface, then the quantity E in (3.18) vanishes. In this case, (3.18) written in terms of the velocity potential takes the form

$$\left[1 - \frac{1}{a^2}\left(\frac{\partial\phi}{\partial x}\right)^2\right]\frac{\partial^2\phi}{\partial x^2} + \left[1 - \frac{1}{a^2}\left(\frac{\partial\phi}{\partial y}\right)^2\right]\frac{\partial^2\phi}{\partial y^2} - \frac{2}{a^2}\,\frac{\partial\phi}{\partial x}\,\frac{\partial\phi}{\partial y}\,\frac{\partial^2\phi}{\partial x\partial y} = 0 \tag{3.20}$$

where

$$a^2 = A + Bq^2$$

with $A = a_0^2 = a_\infty^2 + Bq_\infty^2$, subscripts 0 and ∞ indicating the stagnation point and undisturbed state, $B = (1 - \gamma)/2$, and $q^2 = V_1^2 + V_2^2$.

To proceed with finite element formulations from (3.20), it is convenient to write (3.20) in index notation as follows:

$$\phi,_{ii} - \frac{1}{a^2}\,\phi,_i\phi,_j\phi,_{ij} = 0 \tag{3.21}$$

Setting $\phi = \Phi_N\phi_N$, we obtain the local Galerkin-finite element equation

$$\int_\Omega (\phi,_{ii} - \frac{1}{a^2}\,\phi,_i\phi,_j\phi,_{ij})\Phi_N d\Omega = 0 \tag{3.22}$$

Integrating by parts with first derivatives of ϕ held constant, we get

$$A_{NM}\phi_M = G_N + F_N + S_N \tag{3.23}$$

where

$$A_{NM} = \int_\Omega \Phi_{N,i}\Phi_{M,i}d\Omega \tag{3.24a}$$

$$G_N = \int_\Omega \frac{1}{a^2}\,\Phi_{M,i}\Phi_{P,j}\Phi_{Q,i}\Phi_{N,j}d\Omega\phi_M\phi_P\phi_Q \tag{3.24b}$$

$$F_N = \int_\Gamma \phi,_i n_i \overset{*}{\Phi}_N d\Gamma \tag{3.24c}$$

$$S_N = -\int_\Gamma \frac{1}{a^2}\,\phi,_i\phi,_j\phi,_i n_j \overset{*}{\Phi}_N d\Gamma \tag{3.24d}$$

Here, F_N represents the Neumann boundary conditions on solid surfaces or at free stream, and S_N is the nonlinear boundary condition on the surface or pressure discontinuity, which will be elaborated in Section 3.3. For a shockless domain we set $S_N = 0$. It should be remembered that the partial integration of (3.22) for the nonlinear term is not exact but the momentum is conserved more exactly than the case in which this term is not integrated at all, commonly known as nonconservation form. Note that two of the nonlinear terms can be integrated exactly by setting $\left(\frac{\partial\phi}{\partial x}\right)^2 \frac{\partial^2\phi}{\partial x^2} = \frac{\partial}{\partial x}\left(\frac{1}{3}\left(\frac{\partial\phi}{\partial x}\right)^3\right)$ and $\left(\frac{\partial\phi}{\partial y}\right)^2 \frac{\partial^2\phi}{\partial y^2} = \frac{\partial}{\partial y}\left(\frac{1}{3}\left(\frac{\partial\phi}{\partial y}\right)^3\right)$. In this case, G_N and S_N should be reduced by 2/3 of the integrated values corresponding to these terms. If so, the approximation ($\phi,_i$ held constant) affects only the cross derivative term in (3.20).

For $G_N = S_N = 0$, the equation is reduced to an ideal incompressible flow. The assembled form of (3.21) can be solved using standard techniques for nonlinear equations:

$$A_{ij}\phi_j = G_i + F_i$$

subject to proper boundary conditions. Instead of using techniques such as the Newton-Raphson method, some authors prefer to use a simple iterative procedure by first setting $G_i = 0$ and calculating G_i from the initial solution of ϕ_j. Then G_i is updated for the rest of the iterative cycles until convergence:

$$A_{ij}\phi_j^{(n+1)} = G_i^{(n)} + F_i^{(n)} \tag{3.25}$$

where (n+1) and (n) denote the current and previous iterative cycles.

For simplicity, a less rigorous form based on the small perturbation

theory may be used:

$$(1 - M_\infty^2)\frac{\partial V_1}{\partial x_1} + \frac{\partial V_2}{\partial x_2} + \frac{eV_2}{x_2} = M_\infty^2(1+\gamma)\frac{V_1}{U}\frac{\partial V_1}{\partial x_1}$$

where U is the free stream velocity and $M_\infty = U/a$ is the free stream Mach number. In terms of potential function, we may also write

$$(1 - M_\infty^2)\frac{\partial^2\phi}{\partial x_1^2} + \frac{\partial^2\phi}{\partial x_2^2} + \frac{e}{x_2}\frac{\partial\phi}{\partial x_2} = M_\infty^2\,\frac{(1+\gamma)}{U}\,\frac{\partial\phi}{\partial x_1}\,\frac{\partial^2\phi}{\partial x_1^2} \tag{3.26}$$

This equation is valid for transonic flow. If the right-hand side of (3.26) vanishes, then it is valid for subsonic and supersonic flows.

The pressure coefficients are given approximately (higher order terms neglected) by

$$C_p = -\frac{2V_1}{U} - \frac{eV_2^2}{U^2} \quad \text{or} \quad C_p = -\frac{2}{U}\frac{\partial\phi}{\partial x_1} - \frac{e}{U^2}\left(\frac{\partial\phi}{\partial x_2}\right)^2 \tag{3.27a,b}$$

The finite element equation corresponding to (3.26) is now given by the matrices for two-dimensional flow

$$A_{NM} = \int_\Omega \left(\frac{\partial\Phi_N}{\partial x}\frac{\partial\Phi_M}{\partial x} + \frac{\partial\Phi_N}{\partial y}\frac{\partial\Phi_M}{\partial y}\right) d\Omega \tag{3.28a}$$

$$G_N = \left\{\int_\Omega \left[M_\infty^2 + \frac{1}{2}M_\infty^2\left(\frac{1+\gamma}{U}\right)\frac{\partial\Phi_P}{\partial x}\,\phi_P\right]\frac{\partial\Phi_N}{\partial x}\,\frac{\partial\Phi_M}{\partial x}\,d\Omega\right\}\phi_M \tag{3.28b}$$

$$F_N = \int_\Gamma \left(\frac{\partial\phi}{\partial x}n_1 + \frac{\partial\phi}{\partial y}n_2\right)\overset{*}{\Phi}_N d\Gamma \tag{3.28c}$$

$$S_N = -\int_\Gamma \left[M_\infty^2\frac{\partial\phi}{\partial x} + \frac{1}{2}M_\infty^2\left(\frac{1+\gamma}{U}\right)\left(\frac{\partial\phi}{\partial x}\right)^2\right] n_1\overset{*}{\Phi}_N d\Gamma \tag{3.28d}$$

where $d\Omega = dxdy$. Note that, in contrast to (3.24), G_N and S_N are exactly integrated here. The solution procedure in the small perturbation theory is the same as in (3.23), but with a considerably simpler nonlinear term. The jump condition across the shock waves is satisfied when the integrands

of F_N and S_N are equal or

$$\left[\!\left[(1 - M_\infty^2)\frac{\partial\phi}{\partial x} - \frac{1}{2}M_\infty^2\left(\frac{1+\gamma}{U}\right)\left(\frac{\partial\phi}{\partial x}\right)^2\right]\!\right]n_1 - \left[\!\left[\frac{\partial\phi}{\partial y}\right]\!\right]n_2 = 0$$

where $[\![\cdot]\!]$ denotes the jump and n_1/n_2 is the slope of the discontinuity.

In general, for transonic and supersonic flows around an airfoil, shock waves are expected to develop, thus leading to pressure discontinuities across the shock. Because of the presence of shock waves, solution of the equations presented here will suffer a breakdown. A remedy of this situation as well as general discussions of shock waves will be given in Section 3.3.

3.2 Variational Formulations

The variational principles for compressible flow have been studied by Bateman [18,19] Herivel [20], and Serrin [21], among others. The basic idea of deriving the variational principle in nonlinear equations is to determine the existence of symmetric Fréchet derivative. If the Fréchet is not symmetric, no variational principle exists in general. However, if the flow is irrotational we may use the so-called Bateman principle [18,19] to derive the variational principle for compressible flow,

$$I = \int_\Omega P d\Omega + \int_\Omega f\phi d\Gamma \tag{3.29}$$

where $P = A + B\rho^\gamma$ with A, B, and γ being the constants. The first variation of the integral $\int_\Omega P d\Omega$ attaining the maximum is equivalent to the conservation of mass

$$(\rho V_i)_{,i} = 0 \tag{3.29a}$$

To prove this we begin with the relation of $a^2 = \partial P/\partial \rho$

$$a^2 = B\,\gamma\,\rho^{\gamma-1} = a_\infty^2 + \frac{\gamma-1}{2}(q_\infty^2 - q^2)$$

Denoting $\hat{q}^2 = \dfrac{2a_\infty^2}{\gamma-1} + q_\infty^2$ and neglecting the constants, the variational integral takes the form

$$\int_\Omega (\hat{q}^2 - q^2)^{\frac{\gamma}{\gamma-1}}\, d\Omega = \text{maximum}$$

The first variation of the above becomes

$$\delta I = \delta \int_\Omega (\hat{q}^2 - q^2)^{\frac{\gamma}{\gamma-1}}\, d\Omega = 0$$

With some algebra it can easily be shown that the first variation can be simplified to

$$\delta I = \int_\Omega (\hat{q}^2 - \phi,_j\phi,_j)^{\frac{1}{\gamma-1}}\, \phi,_i\delta\phi,_i\, d\Omega = 0$$

or

$$\delta I = \int_\Omega \rho\phi,_i\delta\phi,_i\, d\Omega = \int_\Omega \left[(\rho\delta\phi\phi,_i),_i - \delta\phi(\rho\phi,_i),_i\right] d\Omega = 0$$

Finally,

$$\delta I = -\int_\Gamma \rho\delta\phi\ \phi,_i n_i d\Gamma - \int_\Omega \delta\phi(\rho\phi,_i),_i\, d\Omega = 0$$

Since $\phi,_i n_i = 0$ or $\delta\phi = 0$ on the boundaries, we now have

$$(\rho\phi,_i),_i = (\rho V_i),_i = 0$$

Thus the validity of (3.29a) has been confirmed.

At this point, we wish to examine the relationship between the variational principle (3.29) and the full potential equation (3.21),

$$\frac{\partial^2\phi}{\partial x^2} + \frac{\partial^2\phi}{\partial y^2} - G(\phi) = 0 \quad \text{in} \quad \Omega \tag{3.30}$$

with

$$G(\phi) = \frac{1}{a^2}\left[\left(\frac{\partial\phi}{\partial x}\right)^2 \frac{\partial^2\phi}{\partial x^2} + 2\,\frac{\partial\phi}{\partial x}\,\frac{\partial\phi}{\partial y}\,\frac{\partial^2\phi}{\partial x\partial y} + \left(\frac{\partial\phi}{\partial y}\right)^2 \frac{\partial^2\phi}{\partial x\partial y}\right]$$

subject to the boundary conditions

$$\phi = g(x,y) \quad \text{on } \Gamma_1$$

$$\phi,_i n_i = 0 \quad \text{on } \Gamma_2$$

If we choose $\gamma = 2$, $a^2 = q^2$ or $\hat{q}^2 = a^2$, and keep the first derivatives $\phi,_i\ \phi,_j$ held constant, then the expression (3.29) can be integrated by parts as follows:

$$\delta I(\phi) = \int_\Omega \left(1 - \frac{1}{a^2}\,\phi,_j\phi,_j\right)\phi,_i\delta\phi,_i \, d\Omega = 0 \tag{3.31a}$$

or

$$\delta I(\phi) = \int_\Gamma \left(\phi,_i n_i - \frac{1}{a^2}\,\phi,_j\phi,_i\phi,_i n_j\right)\delta\phi \, d\Gamma$$
$$- \int_\Omega \left(\phi,_{ii} - \frac{1}{a^2}\,\phi,_i\phi,_j\phi,_{ij}\right)\delta\phi \, d\Omega \tag{3.31b}$$

We notice that the integrand of the last term of (3.31b) becomes zero as it satisfies (3.30). Setting (3.31a) equal to (3.31b), we get

$$\delta I(\phi) = \int_\Omega \left(1 - \frac{1}{a^2}\,\phi,_j\phi,_j\right)\phi,_i\delta\phi,_i \, d\Omega + \int_\Gamma f\delta\phi \, d\Gamma \tag{3.31c}$$

where

$$f = -\,\phi,_i n_i + \frac{1}{a^2}\,\phi,_j\phi,_i\phi,_i n_j$$

The derivation in this context implies that the Bateman principle (3.29) does not lead to the full potential equation (3.30) unless the various assumptions

as proposed here are valid. Rewriting (3.31c) gives

$$\delta I(\phi) = \delta \left[\int_\Omega \frac{1}{2}\left(\phi,_i\phi,_i - \frac{2}{a^2}\phi,_i\phi,_i\phi,_j\phi,_j\right) d\Omega + \int_\Gamma f\phi \, d\Gamma \right] \quad (3.31d)$$

Thus the variational principle valid only under the assumptions made above takes the form

$$I(\phi) = \int_\Omega \left(\frac{1}{2}\phi,_i\phi,_i - \frac{1}{a^2}\phi,_i\phi,_i\phi,_j\phi,_j\right) d\Omega + \int_\Gamma f\phi d\Gamma \quad (3.31e)$$

There are other means of developing the variational principle in an approximate manner using Fréchet differentials [22]. Toward this end, we consider the nonlinear problem

$$N(u) - f = 0$$

and the variational integral

$$I(u,v) = \int_\Omega \left[vN(u) - vf - ug \right] d\Omega$$

The first variation takes the form

$$\delta I = \int_\Omega \left\{ \left[N(u) - f \right] \delta v + \left[\overset{*}{N}(u,v) - g \right] \delta u \right\} d\Omega = 0$$

This may be called an <u>adjoint variational principle</u>. An alternative approach is to write

$$\delta I = \int_\Omega \left[N(u^o) - f \right] \delta u \quad d\Omega = 0$$

in which variations are taken with respect to u while holding u^o constant. Upon the variation we set $u = u^o$ and recover the original governing equation as the "Euler equation." The variational principle of this type is referred to as a <u>restricted variational principle</u> [22]. In this case, the functional is not stationary unless

$$\overset{*}{N}(u,u) - g = 0$$

where $v = u = u^o$. We demonstrate this idea for the compressible flow below.

The derivation of a restricted variational principle for (3.30) begins with

$$\delta I(\phi) = \int_\Omega (\phi,_{ii} - \frac{1}{a^2} \phi,_i\phi,_j\phi,_{ij})\delta\phi d\Omega = 0 \qquad (3.32)$$

With the first derivatives of ϕ in (3.32) held constant, we integrate by parts:

$$\delta I(\phi) = \int_\Gamma \phi,_i n_i \delta\phi d\Gamma - \int_\Omega \phi,_i \delta\phi,_i d\Omega - \int_\Gamma \frac{1}{a^2} \phi,_i\phi,_j\phi,_i n_j \delta\phi d\Gamma$$
$$+ \int_\Omega \frac{1}{a^2} \phi,_i\phi,_j\phi,_i\delta\phi,_j d\Omega$$

or

$$\delta I(\phi) = \delta \int_\Omega \Big[\frac{1}{2} (\phi,_i\phi,_i - \frac{2}{a^2}\phi,_i\phi,_j\phi,_i\phi,_j)\, d\Omega$$
$$- \int_\Gamma \phi,_i n_i \phi d\Gamma + \int_\Gamma \frac{1}{a^2} \phi,_i\phi,_j\phi,_i n_j \phi d\Gamma\Big] \qquad (3.33)$$

The variational functional to be made stationary for the solution of ϕ assumes the form

$$I(\phi) = \int_\Omega \frac{1}{2} \phi,_i\phi,_i d\Omega - \int_\Omega \frac{1}{a^2} \phi,_i\phi,_j\phi,_i\phi,_j d\Omega$$
$$- \int_\Gamma \phi,_i n_i \phi d\Gamma + \int_\Gamma \frac{1}{a^2} \phi,_i\phi,_j\phi,_i n_j \phi d\Gamma \qquad (3.34)$$

The integral $\int_\Gamma \phi,_i n_i \phi d\Gamma$ provides the Neumann boundary condition on solid surfaces whereas the last term of (3.34) denotes the pressure discontinuity. It is interesting to note that (3.34) is identical to (3.31e) as a special case of Bateman principle. In terms of the finite element interpolation

functions, we may write (3.34) in the form

$$I(\phi) = \frac{1}{2} A_{NM}\phi_N\phi_M - B_{NMPQ}\phi_M\phi_P\phi_Q\phi_N - F_N\phi_N + S_N\phi_N \qquad (3.35)$$

Minimizing this functional with respect to the nodal values of the potential yields

$$A_{NM}\phi_M - B_{NMPQ}\phi_M\phi_P\phi_Q - F_N + S_N = 0 \qquad (3.36)$$

Setting the second term equal to G_N, the expression (3.36) is seen to be identical to (3.23).

The finite element solution of the flow around a circular cylinder at low Mach numbers formulated from the pseudo-functional of the type (3.34) was first carried out by Norrie and deVries [23] but without the partial integration of the nonlinear term, resulting in nonconservation form.

An alternate approach proposed by Carey [24] deals with the streamline formulation for two-dimensional, compressible, inviscid, irrotational flow. The governing equation is given by

$$\psi_{,ii}\left[1 + M_\infty^2\left(\frac{\gamma - 1}{2}\right)\right] + G(\psi) = 0 \qquad (3.37)$$

with

$$C(\psi) = \psi_{,ii}\frac{M_\infty^2}{U^2}\left(\frac{\gamma - 1}{2}\right)\varepsilon_{kj}\varepsilon_{k\ell}\psi_{,j}\psi_{,\ell} + \psi_{,i}\frac{M_\infty^2}{U^2}\left(\frac{1}{2}\varepsilon_{kj}\varepsilon_{k\ell}\psi_{,j}\psi_{,\ell}\right)_{,i} = 0 \qquad (3.38)$$

Although Carey utilizes the perturbation expansion of ψ, it may be simpler to follow the procedure for the pseudo-variational functional approach as demonstrated for the velocity potential. This takes the form

$$\delta I(\psi) = \int_\Omega \left\{\nabla^2\psi\left[1 + M_\infty^2\left(\frac{\gamma - 1}{2}\right)\right] + G(\psi)\right\}\delta\psi d\Omega \qquad (3.39)$$

Thus the variational principle (holding $\psi,_j\psi,_\ell$ constant) is derived as

$$I(\psi) = \int_\Omega \left\{\frac{1}{2}\,\psi,_i\psi,_i\left[1 + M_\infty^2\left(\frac{\gamma - 1}{2}\right)\right] - \frac{1}{2}\frac{M_\infty^2}{U^2}\left(\frac{\gamma + 1}{2}\right)\varepsilon_{kj}\varepsilon_{k\ell}\psi,_i\psi,_i\psi,_j\psi,_\ell\right\} d\Omega$$
$$- \int_\Gamma \left\{\psi,_i n_i \psi - \frac{M_\infty^2}{U^2}\left(\frac{\gamma + 1}{2}\right)\varepsilon_{kj}\varepsilon_{k\ell}\psi,_i\psi,_j\psi,_\ell n_i \psi\right\} d\Gamma \qquad (3.40)$$

With suitable finite element interpolation functions, we can write (3.40) in the form

$$I(\psi) = \frac{1}{2} A_{NM}\psi_N\psi_M - B_{NMPQ}\psi_N\psi_M\psi_P\psi_Q - F_N\psi_N + S_N\psi_N \qquad (3.41)$$

The corresponding finite element equation becomes

$$A_{NM}\psi_M - B_{NMPQ}\psi_M\psi_P\psi_Q - F_N + S_N = 0 \qquad (3.42)$$

with the appearance of this equation identical to that for the velocity potential formulation (3.37).

Carey [24], using the form (3.37) together with the perturbation expansion of ψ instead of the approach (3.42), presents the finite element solution of the fully-infinite compressible flow past a cylinder. Note that in the perturbation solution, the Laplace equation is solved first and the further solutions repeated with effects of compressibility added, the basic idea being similar to the solution of (3.42) in which the first term refers to the incompressible flow whereas the second term represents a compressibility correction.

3.3 Transonic Aerodynamics

3.3.1 General

Transonic gas flows are governed by partial differential equations of mixed types. The theory was initiated in the historical memoir of

Tricomi [25] in the form

$$y \frac{\partial^2\phi}{\partial x^2} + \frac{\partial^2\phi}{\partial y^2} = 0 \tag{3.43}$$

which is hyperbolic for $y < 0$ and elliptic for $y > 0$.

The extreme lateral influence produced by an obstacle in a stream near Mach number unity may be studied by the linearized equation for two-dimensional flow with small perturbations,

$$(1 - M_\infty^2) \frac{\partial^2\phi}{\partial y^2} + \frac{\partial^2\phi}{\partial y^2} = 0 \tag{3.44}$$

This shows that when $M_\infty = 1$, we have $\frac{\partial^2\phi}{\partial y^2} = 0$, and therefore the perturbation velocity $V_y = \frac{\partial\phi}{\partial y}$ depends only on x. This implies that the disturbance produced by the body is propagated laterally with undiminished strength. Since the curvature of the streamlines remains finite as y increases, it follows that infinite pressure differences can exist between the surface of the body and points at great lateral distances from the body. Thus, the linear theory invalidates the physical conditions and we may resort to the nonlinear theory of small perturbation,

$$(1 - M_\infty^2) \frac{\partial^2\phi}{\partial x^2} + \frac{\partial^2\phi}{\partial y^2} = M_\infty^2 \frac{(1 + \gamma)}{U} \frac{\partial\phi}{\partial x} \frac{\partial^2\phi}{\partial x^2} \tag{3.45}$$

or the more rigorous and general equation of transonic flow,

$$(a^2 - u^2) \frac{\partial u}{\partial x} + (a^2 - v^2)\frac{\partial v}{\partial y} - 2uv \frac{\partial u}{\partial y} = 0 \tag{3.46}$$

Written alternatively,

$$\nabla^2\phi - G = 0 \tag{3.47}$$

with

$$G = \frac{1}{a^2}\left[\left(\frac{\partial\phi}{\partial x}\right)^2 \frac{\partial^2\phi}{\partial x^2} + 2 \frac{\partial\phi}{\partial x} \frac{\partial\phi}{\partial y} \frac{\partial^2\phi}{\partial x\partial y} + \left(\frac{\partial\phi}{\partial y}\right)^2 \frac{\partial^2\phi}{\partial y^2}\right]$$

For unsteady conditions, the small perturbation theory provides

$$\frac{\partial^2\phi}{\partial x^2} + \frac{\partial^2\phi}{\partial y^2} - 2M_\infty^2 \frac{\partial}{\partial t}\left(\frac{\partial\phi}{\partial x}\right) - M_\infty^2 \frac{\partial^2\phi}{\partial t^2} - G = 0 \qquad (3.48)$$

with

$$G = M_\infty^2 + M_\infty^2 \frac{(1+\gamma)}{U} \frac{\partial\phi}{\partial x} \frac{\partial^2\phi}{\partial x^2}$$

If the amplitude of airfoil oscillation is small in comparison with the airfoil thickness, it is possible to linearize the unsteady problem by taking $\hat{\phi}$ to be a small perturbation on ϕ. This gives the following linearized differential equation for $\hat{\phi}$ in nondimensionalized form:

$$(1 - M_\infty^2)\frac{\partial^2\hat{\phi}}{\partial x^2} - M_\infty^2(\gamma+1)\frac{\partial}{\partial x}\left(\frac{\partial\phi}{\partial x}\frac{\partial\hat{\phi}}{\partial x}\right) + \frac{\partial^2\hat{\phi}}{\partial y^2} + \frac{e}{y}\frac{\partial\hat{\phi}}{\partial y} - 2M_\infty^2\frac{\partial}{\partial t}\left(\frac{\partial\hat{\phi}}{\partial x}\right) - M_\infty^2\frac{\partial^2\hat{\phi}}{\partial t^2} = 0 \qquad (3.49)$$

with $x = x'/a$, $y = y'/a$, $t = t'U/a$, $\phi = \phi'/Ua$.

For the flow over a harmonically oscillating body, we set

$$\hat{\phi} = R_e\left[\bar{\phi}e^{ikt}\right] \qquad (3.50)$$

where $\bar{\phi}$ is a complex function and k is the frequency of oscillation. Substituting (3.50) into (3.49) yields

$$(1 - M_\infty^2)\frac{\partial^2\bar{\phi}}{\partial x^2} - M_\infty^2(\gamma+1)\frac{\partial}{\partial x}\left(\frac{\partial\phi}{\partial x}\frac{\partial\bar{\phi}}{\partial x}\right) + \frac{\partial^2\bar{\phi}}{\partial y^2} + \frac{e}{y}\frac{\partial\bar{\phi}}{\partial y} - 2ikM_\infty^2\frac{\partial\bar{\phi}}{\partial x} + k^2M_\infty^2\bar{\phi} = 0$$

with $i = \sqrt{-1}$

The physics represented by these equations is predicted reasonably well qualitatively. Some significant quantitative results from wind tunnel experiments are also available. Shock waves are an essential feature of transonic flow and their appearance on a moving body leads to a rapid increase in drag coefficient with increasing Mach numbers.

The analytical solution of the nonlinear-mixed type equations is a formidable task. In recent years, significant achievements have been made by workers on computational fluid dynamics using the method of finite difference. The finite difference method in shock wave problems was studied by von Neumann and Richtmyer [26], among others. They introduced an artificial dissipative mechanism so that the shock transition would become smooth without the necessity of shock fitting [27] in which the incomplete information by the jump conditions must be supplemented by additional information coming to the shock from the fluid behind it. Since the shock-fitting technique often breaks down when shocks develop spontaneously within the fluid, von Neumann and Richtmyer avoided the direct use of the Hugoniot jump conditions but retained the basic conservation laws on which the Hugoniot conditions are based, in which the jump conditions still hold across the transition layer. Specifically, the dissipative mechanisms such as viscosity and heat conduction are included so that the surface of discontinuity is replaced by a thin transition layer in which quantities change rapidly, not discontinuously. The Hugoniot relations are satisfied such that the "smeared-out" shock travels with exactly the same speed as a discontinuous one would.

Alternative forms of the viscosity term have been proposed by a number of researchers such as Lax-Wendroff [28], MacCormack [29], and Murman and Cole [30], among others. In the recent works of Jameson [31], the conservation equations are centrally differenced for subsonic region and upwind differenced for the supersonic region for better representation of shock waves, Wellford and Oden [32] presented the finite element applications to shock waves in solids. In these works, the derivative of the axial

displacement is defined in terms of an unknown distance at which a shock front travels. The finite element with such discontinuity may be termed "moving shock element". In the flow field around a body, however, a shock is at least two-dimensional. Our attention is focused on whether there is a shock discontinuity at any given location and time. With this in mind, we introduce here a special finite element referred to as the "stationary shock element" [33].

3.3.2 Element Discontinuity Method for Shock Waves

Let us assume that the shock wave passes through an element causing a pressure jump. Here we consider an explicit discontinuity at the center of the isoparametric element as depicted in Fig. 3.1. An independent interpolation of ϕ for each quadrant is given by (Fig. 3.2)

$$\phi^{(\alpha)} = \alpha_1 + \alpha_2\xi + \alpha_3\eta + \alpha_4\xi\eta + \alpha_5\xi^2 + \alpha_6\eta^2 \tag{3.52a}$$

$$\phi^{(\beta)} = \beta_1 + \beta_2\xi + \beta_3\eta + \beta_4\xi\eta + \beta_5\xi^2 + \beta_6\eta^2 \tag{3.52b}$$

$$\phi^{(\gamma)} = \gamma_1 + \gamma_2\xi + \gamma_3\eta + \gamma_4\xi\eta + \gamma_5\xi^2 + \gamma_6\eta^2 \tag{3.52c}$$

$$\phi^{(\delta)} = \delta_1 + \delta_2\xi + \delta_3\eta + \delta_4\delta\eta + \delta_5\xi^2 + \delta_6\eta^2 \tag{3.52d}$$

Here we introduce a total of 24 constants to be determined uniquely. Return to the equation (3.52), we may write 4 equations for ϕ at the corner nodes, 8 equations for ϕ at the midside nodes, and 4 equations for ϕ at the center node, resulting in 16 equations. We obtain 8 additional equations for the difference between the slopes of ϕ and their rates of change at the center node. They are

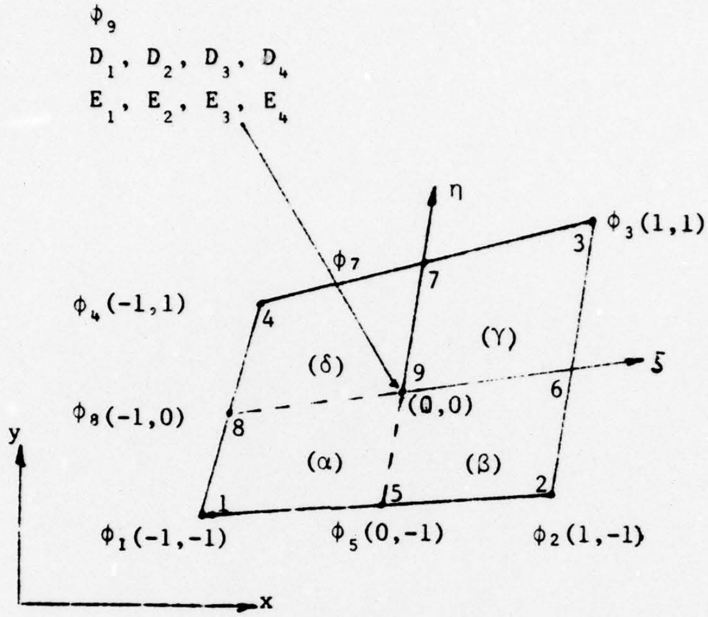

Figure 3.1 Isoparametric Element

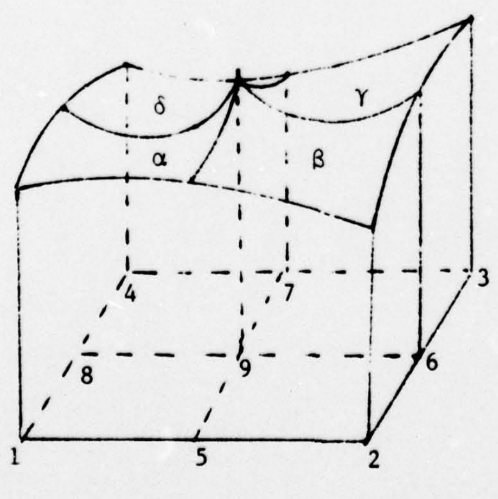

Figure 3.2 Representation of Discontinuous Functions

$$D_1 = \frac{\partial\phi^{(\alpha)}}{\partial\xi} - \frac{\partial\phi^{(\beta)}}{\partial\xi}, \quad D_2 = \frac{\partial\phi^{(\beta)}}{\partial\eta} - \frac{\partial\phi^{(\gamma)}}{\partial\eta}, \quad D_3 = \frac{\partial\phi^{(\gamma)}}{\partial\xi} - \frac{\partial\phi^{(\delta)}}{\partial\xi}, \quad D_4 = \frac{\partial\phi^{(\delta)}}{\partial\eta} - \frac{\partial\phi^{(\alpha)}}{\partial\eta}$$

$$E_1 = \frac{\partial^2\phi^{(\alpha)}}{\partial\xi^2} - \frac{\partial^2\phi^{(\beta)}}{\partial\xi^2}, \quad E_2 = \frac{\partial^2\phi^{(\beta)}}{\partial\eta^2} - \frac{\partial^2\phi^{(\gamma)}}{\partial\eta^2}, \quad E_3 = \frac{\partial^2\phi^{(\gamma)}}{\partial\xi^2} - \frac{\partial^2\phi^{(\delta)}}{\partial\xi^2}, \quad E_4 = \frac{\partial^2\phi^{(\delta)}}{\partial\eta^2} - \frac{\partial^2\phi^{(\alpha)}}{\partial\eta^2} \tag{3.53}$$

With these 24 equations now available, we solve for the unknown constants to be substituted back into (3.52). Thus we have

$$\phi^{(\alpha)} = \Phi_N^{(\alpha)}(\xi,\eta)\phi_N + F_r^{(\alpha)}(\xi,\eta)D_r + G_r^{(\alpha)}(\xi,\eta)E_r$$

$$\phi^{(\beta)} = \Phi_N^{(\beta)}(\xi,\eta)\phi_N + F_r^{(\beta)}(\xi,\eta)D_r + G_r^{(\beta)}(\xi,\eta)E_r$$

$$\phi^{(\gamma)} = \Phi_N^{(\gamma)}(\xi,\eta)\phi_N + F_r^{(\gamma)}(\xi,\eta)D_r + G_r^{(\gamma)}(\xi,\eta)E_r$$

$$\phi^{(\delta)} = \Phi_N^{(\delta)}(\xi,\eta)\phi_N + F_r^{(\delta)}(\xi,\eta)D_r + G_r^{(\delta)}(\xi,\eta)E_r$$

where $N = 1,2,\ldots,9$ and $r = 1,2,3,4$. It is clear that Φ_N, F_r, and G_r represent the interpolation functions for continuity of ϕ_N and discontinuities of D_r and E_r, respectively (See Table 3.1).

To obtain the finite element analogue of (3.47), we assure an interpolation field for the velocity potential function in the form

$$\phi = \Psi_m Q_m \tag{3.54}$$

Here Ψ_m represent the continuous interpolation functions for ϕ and the discontinuous interpolation functions for derivatives of ϕ at the element nodes; Q_m denote the nodal values of ϕ plus its first and possibly second order discontinuous derivatives. An orthogonal projection of the residuals of (3.47) onto the subspace spanned by both continuous and discontinuous interpolation fields leads to

$$\int_\Omega (\phi,_{ii} - G)\Psi_m d\Omega = 0 \tag{3.55}$$

	(α)	(β)	(γ)	(δ)
Φ_1	$\xi\eta$	0	0	0
Φ_2	0	$-\xi\eta$	0	0
Φ_3	0	0	$\xi\eta$	0
Φ_4	0	0	0	$-\xi\eta$
Φ_5	$-1/2(\eta+2\xi\eta-\eta^2)$	$-1/2(\eta-2\xi\eta-\eta^2)$	$-1/2(\eta-\eta^2)$	$-1/2(\eta+\eta^2)$
Φ_6	$1/2(\xi+\xi^2)$	$1/2(\xi+2\xi\eta+\xi^2)$	$1/2(\xi-2\xi\eta+\xi^2)$	$1/2(\xi+\xi^2)$
Φ_7	$1/2(\eta+\eta^2)$	$1/2(\eta+\eta^2)$	$1/2(\eta-2\xi\eta+\eta^2)$	$1/2(\eta+2\xi\eta+\eta^2)$
Φ_8	$-1/2(\xi+2\xi\eta-\xi^2)$	$-1/2(\xi-\xi^2)$	$-1/2(\xi-\xi^2)$	$-1/2(\xi-2\xi\eta-\xi^2)$
Φ_9	$1+\xi\eta-\xi^2-\eta^2$	$1-\xi\eta-\xi^2-\eta^2$	$1+\xi\eta-\xi^2-\eta^2$	$1-\xi\eta-\xi^2-\eta^2$
F_1	$1/2(\xi+\xi^2)$	$-1/2(\xi-\xi^2)$	0	0
F_2	0	$1/2(\eta+\eta^2)$	$-1/2(\eta-\eta^2)$	0
F_3	0	0	$1/2(\xi-\xi^2)$	$-1/2(\xi+\xi^2)$
F_4	$-1/2(\eta+\eta^2)$	0	0	$1/2(\eta-\eta^2)$
G_1	$1/4(\xi+\xi^2)$	$1/4(\xi-\xi^2)$	0	0
G_2	0	$1/4(\eta+\eta^2)$	$1/4(\eta-\eta^2)$	0
G_3	0	0	$-1/4(\xi-\xi^2)$	$-1/4(\xi+\xi^2)$
G_4	$-1/4(\eta+\eta^2)$	0	0	$-1/4(\eta-\eta^2)$

Table 3.1 Interpolation Functions

which is identical to (3.22) except for the new test functions Ψ_m replacing the standard interpolation functions Φ_N. Integrating by parts yields

$$A_{mn} Q_n = G_m + F_m + S_m \tag{3.56}$$

where

$$A_{mn} = \int_\Omega \Psi_{m,i} \Psi_{n,i} d\Omega \tag{3.57}$$

$$G_m = \int_\Omega \frac{1}{a^2} \Psi_{n,i} \Psi_{p,j} \Psi_{q,i} \Psi_{m,j} d\Omega Q_n Q_p Q_q \tag{3.58}$$

$$F_m = \int_{\Gamma_1} \phi,_i n_i \overset{*}{\Psi}_m d\Gamma \tag{3.59}$$

$$S_m = -\int_{\Gamma_2} \beta_j n_n \overset{*}{\Psi}_m d\Gamma \tag{3.60}$$

with $\beta_j = \frac{1}{a^2} \phi,_i \phi,_j \phi,_i$. For the small perturbation theory, these matrices are of the form (3.24), now equipped with shock element interpolation functions instead of Φ_N. The boundary conditions are given by F_m representing the Neumann type on Γ_1, and S_m denoting the surfaces of pressure discontinuity on Γ_2 as shown in Fig. 3.3. We introduce a notation for discontinuity given by (3.60):

$$S_m = (S_m)_1 - (S_m)_2 \tag{3.61}$$

where the subscripts 1 and 2 refer to the upstream and downstream values of S_m, respectively, at the surface of pressure discontinuity.

From the element geometry (Fig. 3.1), we find that a typical 17 x 17 shock element influence coefficient matrix A_{mn} takes the form

$$\begin{aligned} A_{mn} &= \int_\Omega \left(\frac{\partial \Psi_m}{\partial x} \frac{\partial \Psi_n}{\partial x} + \frac{\partial \Psi_m}{\partial y} \frac{\partial \Psi_n}{\partial y} \right) d\Omega \\ &= \int_{-1}^{0}\int_{-1}^{0} \frac{\partial \Psi_m^{(\alpha)}}{\partial x} \frac{\partial \Psi_n^{(\alpha)}}{\partial x} |J| d\xi d\eta + \int_{-1}^{0}\int_{0}^{0} \frac{\partial \Psi_m^{(\beta)}}{\partial x} \frac{\partial \Psi_n^{(\beta)}}{\partial x} |J| d\xi d\eta \\ &= \int_{0}^{1}\int_{0}^{1} \frac{\partial \Psi_m^{(\gamma)}}{\partial x} \frac{\partial \Psi_n^{(\gamma)}}{\partial x} |J| d\xi d\eta + \int_{0}^{1}\int_{-1}^{0} \frac{\partial \Psi_m^{(\delta)}}{\partial x} \frac{\partial \Psi_n^{(\delta)}}{\partial x} |J| d\xi d\eta + \ldots \end{aligned} \tag{3.62}$$

$$\frac{\partial \psi_m^{(\alpha)}}{\partial x} = \frac{1}{|J|}\left(\frac{\partial y}{\partial \eta}\frac{\partial \psi_m^{(\alpha)}}{\partial \xi} - \frac{\partial y}{\partial \xi}\frac{\partial \psi_m^{(\alpha)}}{\partial \eta}\right)$$, etc., with $x = \Lambda_N x_N$ and $y = \Lambda_N y_N$,

Λ_N being the standard isoparametric interpolation function derived from

$$x,y = c_1 + c_2\xi + c_3\eta + c_4\xi\eta + c_5\xi^2 + c_6\eta^2 + c_7\xi^2\eta + c_8\xi\eta^2 + c_9\xi^2\eta^2,$$

and

$$|J| = \frac{\partial x}{\partial \xi}\frac{\partial y}{\partial \eta} - \frac{\partial x}{\partial \eta}\frac{\partial y}{\partial \xi} \tag{3.63}$$

$$\psi_m^{(\alpha)} = [\Phi_1\ \Phi_2\ \ldots.\ \Phi_9 F_1 F_2 F_3 F_4 G_1 G_2 G_3 G_4]^{(\alpha)}$$

$$\psi_m^{(\beta)} = [\Phi_1\ \Phi_2\ \ldots.\ \Phi_9 F_1 F_2 F_3 F_4 G_1 G_2 G_3 G_4]^{(\beta)}$$

$$\psi_m^{(\gamma)} = [\Phi_1\ \Phi_2\ \ldots.\ \Phi_9 F_1 F_2 F_3 F_4 G_1 G_2 G_3 G_4]^{(\gamma)}$$

$$\psi_m^{(\delta)} = [\Phi_1\ \Phi_2\ \ldots.\ \Phi_9 F_1 F_2 F_3 F_4 G_1 G_2 G_3 G_4]^{(\delta)}$$

$$Q_m = [\phi_1\ \phi_2\ \ldots.\ \phi_9 D_1 D_2 D_3 D_4 E_1 E_2 E_3 E_4]^T$$

The Gaussian quadrature integration of the type (3.62) is also performed on the nonlinear term G_m. Thus the globally assembled finite element equations are written as

$$A_{\alpha\beta} Q_\beta = G_\alpha + F_\alpha + S_\alpha \tag{3.64}$$

Here the Neumann boundary conditions F_α can be satisfied automatically, but we require special treatment for the shock conditions S_α. Toward this end, we resort to direct applications of Rankine-Hugoniot conditions (see Fig. 3.4) to obtain an equivalent form of S_α. The Rankine-Hugoniot conditions are:

$$\rho_1 u_{n1} = \rho_2 u_{n2}$$

together with momentum normal and tangent to the wave,

$$\rho_1 u_{n1}^2 + P_1 = \rho_2 u_{n2}^2 + P_2$$

$$u_{t1} = u_{t2}$$

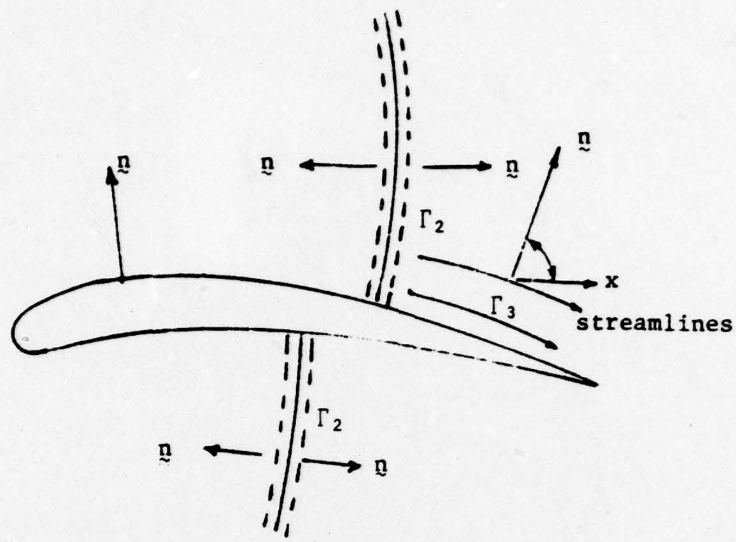

Figure 3.3 Boundary Surfaces

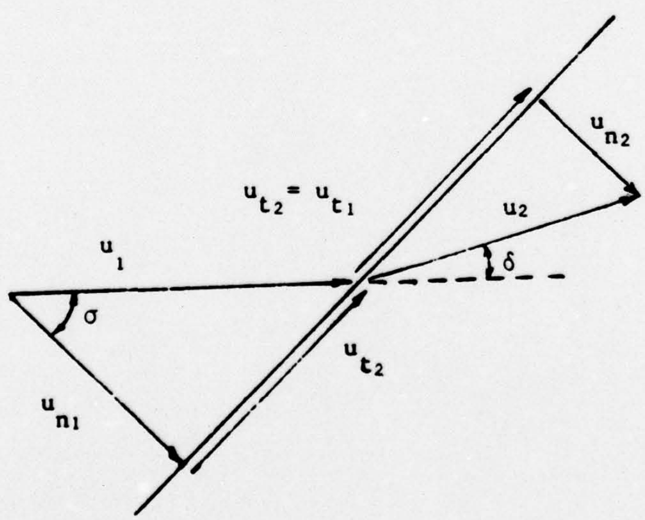

Figure 3.4 Rankine-Hugoniot Conditions

and the energy

$$H_1 + \frac{1}{2} u_1^2 = H_2 + \frac{1}{2} u_2^2 = \hat{H}$$

These equations, in view of the geometric relations and the appropriate equations of state, lead to [34],

$$1 - \varepsilon = A$$

with $A = (1 - \varepsilon_1)(1 - d)$

$$\varepsilon = u_{n2}/u_{n1}, \quad \varepsilon_1 = \frac{\gamma - 1}{\gamma + 1} + \frac{2}{(\gamma + 1)M_1^2} = \frac{a_*^2}{u_1^2}$$

$$d = \tan^2\sigma/(M_1^2 - 1), \quad a_*^2 = \frac{\gamma - 1}{\gamma + 1}\left(1 + \frac{2}{(\gamma - 1)M_\infty^2}\right)\hat{U}^2$$

Thus the Rankine-Hugoniot condition results in

$$(1 - A)u_{n1} - u_{n2} = 0$$

or

$$\left[(1 - A)\cos\sigma - \frac{\sin\sigma}{\tan(\sigma + \delta)}\right] u_1 = 0 \tag{3.65a}$$

This can be easily recast in the form

$$q_{k\alpha} Q_\alpha = 0 \tag{3.65b}$$

Here u_1 is the resultant local velocity upstream of the oblique shock. The shock angle σ is determined from the discontinuity values D_r at the element center. Note that the downstream velocity u_2 is eliminated through the deflection angle δ, which is determined between the tangential velocity u_{t2} and the downstream velocity u_2. The shock boundary condition matrix (3.65b) is now equivalent to (3.61). The quantity $q_{k\alpha}$ is called the shock boundary matrix with k denoting the number of shock elements.

To enforce the shock boundary condition (3.65b), we make use of Lagrange multipliers λ_k such that

$$\lambda_k\, q_{k\alpha} Q_\alpha = 0 \tag{3.66}$$

To replace S_α in (3.64) through the Lagrange multipliers, we construct an energy functional in quadratic form

$$\chi = \frac{1}{2} A_{\alpha\beta} Q_\alpha Q_\beta - R_\alpha Q_\alpha \tag{3.67}$$

where $R_\alpha = G_\alpha + F_\alpha$. Adding (3.66) to (3.67), we obtain

$$\chi = \frac{1}{2} A_{\alpha\beta} Q_\alpha Q_\beta - R_\alpha Q_\alpha + \lambda_k q_{k\alpha} Q_\alpha \tag{3.68}$$

Our objective is to seek an extremum of χ for the flow field satisfying the jump conditions with respect to every Q_α and λ_k,

$$\delta\chi = \frac{\partial\chi}{\partial Q_\alpha}\, \delta Q_\alpha + \frac{\partial\chi}{\partial\lambda_k}\, \delta\lambda_k = 0$$

For all arbitrary values of δQ_α and $\delta\chi_k$, we must have $\frac{\partial\chi}{\partial Q_\alpha} = 0$ and $\frac{\partial\chi}{\partial\lambda_k} = 0$, leading to

$$\begin{bmatrix} A_{\alpha\beta} & q_{k\alpha} \\ q_{k\beta} & 0 \end{bmatrix} \begin{bmatrix} Q_\beta \\ \lambda_k \end{bmatrix} = \begin{bmatrix} R_\alpha \\ 0 \end{bmatrix} \tag{3.69}$$

Writing (3.69) in a compact form

$$B_{ij} X_j = Y_i \tag{3.70}$$

and noting that Y_i contains R_α which is nonlinear, we may cast (3.70) in an iterative form

$$B_{ij} X_j^{(n+1)} = Y_i^{(n)} \tag{3.71a}$$

Initially, we consider a shockless domain, with $R_\alpha = 0$:

$$A_{\alpha\beta} Q_\beta = 0 \tag{3.71b}$$

If the solution (3.71) yields Q_β indicating nonzero D_r, then (3.71) will be replaced by the expression containing the jump condition (3.69) in the

subsequent iterations. In this iterative scheme R will be kept updated.

The magnitude of D_r calculated at the center of an element signifies the strength of the shock. The direction of the shock is determined by connecting the centers of shock elements ($D_r \neq 0$). For multiple occurrences, interactions, and reflections of shocks, it is advisable to start with the shock element influence coefficients applied to the entire domain. At each iterative cycle, we remove the shock boundary matrix $q_{k\alpha}$ when D_r is found to be zero,

$$A_{\alpha\beta}Q_{\beta} = R_{\alpha}$$

In the interest of simplified iterative calculations, the expression (3.55) may be written in a global form as

$$\int_{\Omega} \left(\phi,_{ii} - \left(\frac{q}{a}\right)^2 \phi,_{ii}\right) \Psi_{\alpha} d\Omega = 0 \qquad (3.72a)$$

This leads to

$$A_{\alpha\beta}Q_{\beta} = G_{\alpha} + F_{\alpha} + S_{\alpha} \qquad (3.72b)$$

where

$$G_{\alpha} = K^2 \left[\int_{\Omega} \Psi_{\alpha,i}\Psi_{\beta,i} d\Omega\right] Q_{\beta}$$

$$S_{\alpha} = K^2 \int_{\Gamma} \Psi,_{i} n_{i} \overset{*}{\Psi}_{\alpha} d\Gamma$$

$$K^2 = \left(\frac{q}{a}\right)^2$$

with other quantities being the same as in (3.64). Notice that the quantity K^2 is to be held constant during each iterative cycle and updated for the following cycles. Had we used the Bateman principle with $\gamma = 2$, then we have

$K^2 = (q/\hat{q})$ with

$$\hat{q}^2 = \frac{2a_{\infty}^2}{\gamma-1} + q_{\infty}^2$$

Once again, the shock surface boundary condition S_α is replaced by the Rankine-Hugoniot condition through the Lagrange multipliers (3.65). Otherwise, the finite element equations (3.72) are identical to those derived from (3.29) or (3.31).

If the entropy and enthalpy gradients are non-vanishing normal to the streamlines, then we need to modify (3.55) in the form

$$\int_\Omega (\nabla^2\phi - G - E)\Psi_m d\Omega = 0 \tag{3.73}$$

with E given by (3.19),

$$\begin{aligned} E &= \frac{uv}{\varepsilon_{ij}V_j n_i}\left(\frac{1}{\gamma R}\,\eta_{,i}n_i - \frac{1}{a^2}\hat{H}_{,i}n_i\right) \\ &= \frac{uv}{u\cos\theta - v\sin\theta}\left\{\left(\frac{c_v}{\gamma RP} - \frac{\gamma}{a^2(\gamma-1)\rho}\right)\left(\frac{\partial P}{\partial x}\cos\theta + \frac{\partial P}{\partial y}\sin\theta\right)\right. \\ &\quad + \left(\frac{\gamma P}{a^2(\gamma-1)} - \frac{c_v}{R\rho}\right)\left(\frac{\partial \rho}{\partial x}\cos\theta + \frac{\partial \rho}{\partial y}\sin\theta\right) - \frac{1}{a^2}\left[u\left(\frac{\partial u}{\partial x}\cos\theta + \frac{\partial u}{\partial y}\sin\theta\right)\right. \\ &\quad \left.\left. + v\left(\frac{\partial v}{\partial x}\cos\theta + \frac{\partial v}{\partial y}\sin\theta\right)\right]\right\} \end{aligned} \tag{3.74}$$

where the angle θ is measured between the x axis and the direction normal to the streamlines. In this case, the velocity vector is given by

$$\underset{\sim}{V} = \underset{\sim}{\nabla}\phi + \underset{\sim}{\nabla}\times\underset{\sim}{\phi}$$

Here $\underset{\sim}{\phi}$ is the vector potential. This situation is represented by $E \neq 0$ or the entropy and enthalpy gradient vector-

$$E_m = \int_{\Gamma_3} E\overset{*}{\Psi}_m d\Gamma \neq 0$$

which is added to (3.56):

$$A_{mn}Q_n = G_m + F_m + E_m + S_m \tag{3.75}$$

The entropy and enthalpy gradient vector is calculated from the relation between the pressure-density and the local velocity distribution, lagging

one step behind the iterative solution. It is observed that the enthalpy gradients in general are negligible. Direction cosines are determined from the angles between the x axis and the direction normal to the streamline which corresponds to the equipotential line.

The 17 x 17 element coefficient matrix is rather large in size and it may be advantageous to condense it to a smaller size via standard condensation schemes. We also note that the Gaussian quadrature integration must be performed within each element requiring the half interval. An alternative approach is to provide an independent interpolation field for each quandrant so that the Gaussian integration limits run -1 to 1. In this scheme, we provide at the center node two first derivatives of ϕ for each quadrant, $\partial\phi^{(\alpha)}/\partial\xi$ and $\partial\phi^{(\alpha)}/\partial\eta$, etc. Together with 4 nodal ϕ values, there are 6 generalized coordinates for each quadrant. Thus the interpolation fields are modified to

$$
\begin{aligned}
\phi^{(\alpha)} &= \Phi_1^{(\alpha)}\phi_1 + \Phi_5^{(\alpha)}\phi_5 + \Phi_8^{(\alpha)}\phi_8 + \Phi_9^{(\alpha)}\phi_9 + F_\xi^{(\alpha)}\left(\frac{\partial\phi}{\partial\xi}\right)_9^{(\alpha)} + F_\eta^{(\alpha)}\left(\frac{\partial\phi}{\partial\eta}\right)_9^{(\alpha)} \\
\phi^{(\beta)} &= \Phi_2^{(\beta)}\phi_2 + \Phi_5^{(\beta)}\phi_5 + \Phi_6^{(\beta)}\phi_6 + \Phi_9^{(\beta)}\phi_9 + F_\xi^{(\beta)}\left(\frac{\partial\phi}{\partial\xi}\right)_9^{(\beta)} + F_\eta^{(\beta)}\left(\frac{\partial\phi}{\partial\eta}\right)_9^{(\beta)} \\
\phi^{(\gamma)} &= \Phi_3^{(\gamma)}\phi_3 + \Phi_6^{(\gamma)}\phi_6 + \Phi_7^{(\gamma)}\phi_7 + \Phi_9^{(\gamma)}\phi_9 + F_\xi^{(\gamma)}\left(\frac{\partial\phi}{\partial\xi}\right)_9^{(\gamma)} + F_\eta^{(\gamma)}\left(\frac{\partial\phi}{\partial\eta}\right)_9^{(\gamma)} \\
\phi^{(\delta)} &= \Phi_4^{(\delta)}\phi_4 + \Phi_7^{(\delta)}\phi_7 + \Phi_8^{(\delta)}\phi_8 + \Phi_9^{(\delta)}\phi_9 + F_\xi^{(\delta)}\left(\frac{\partial\phi}{\partial\xi}\right)_9^{(\delta)} + F_\eta^{(\delta)}\left(\frac{\partial\phi}{\partial\eta}\right)_9^{(\delta)}
\end{aligned}
\tag{3.76}
$$

Now each quadrant can be treated as an independent element having the size 6 x 6. In the assembly, ϕ is common to all quadrants at the center node whereas all the second derivative terms remain as generalized coordinates, independent of adjacent quadrants. In this approach, although the shock strengths are not directly calculated, the definitions given in (3.53)

one step behind the iterative solution. It is observed that the enthalpy gradients in general are negligible. Direction cosines are determined from the angles between the x axis and the direction normal to the streamline which corresponds to the equipotential line.

The 17 x 17 element coefficient matrix is rather large in size and it may be advantageous to condense it to a smaller size via standard condensation schemes. We also note that the Gaussian quadrature integration must be performed within each element requiring the half interval. An alternative approach is to provide an independent interpolation field for each quandrant so that the Gaussian integration limits run -1 to 1. In this scheme, we provide at the center node two first derivatives of ϕ for each quadrant, $\partial\phi^{(\alpha)}/\partial\xi$ and $\partial\phi^{(\alpha)}/\partial\eta$, etc. Together with 4 nodal ϕ values, there are 6 generalized coordinates for each quadrant. Thus the interpolation fields are modified to

$$\begin{aligned}
\phi^{(\alpha)} &= \Phi_1^{(\alpha)}\phi_1 + \Phi_5^{(\alpha)}\phi_5 + \Phi_8^{(\alpha)}\phi_8 + \Phi_9^{(\alpha)}\phi_9 + F_\xi^{(\alpha)}\left(\frac{\partial\phi}{\partial\xi}\right)_9^{(\alpha)} + F_\eta^{(\alpha)}\left(\frac{\partial\phi}{\partial\eta}\right)_9^{(\alpha)} \\
\phi^{(\beta)} &= \Phi_2^{(\beta)}\phi_2 + \Phi_5^{(\beta)}\phi_5 + \Phi_6^{(\beta)}\phi_6 + \Phi_9^{(\beta)}\phi_9 + F_\xi^{(\beta)}\left(\frac{\partial\phi}{\partial\xi}\right)_9^{(\beta)} + F_\eta^{(\beta)}\left(\frac{\partial\phi}{\partial\eta}\right)_9^{(\beta)} \\
\phi^{(\gamma)} &= \Phi_3^{(\gamma)}\phi_3 + \Phi_6^{(\gamma)}\phi_6 + \Phi_7^{(\gamma)}\phi_7 + \Phi_9^{(\gamma)}\phi_9 + F_\xi^{(\gamma)}\left(\frac{\partial\phi}{\partial\xi}\right)_9^{(\gamma)} + F_\eta^{(\gamma)}\left(\frac{\partial\phi}{\partial\eta}\right)_9^{(\gamma)} \\
\phi^{(\delta)} &= \Phi_4^{(\delta)}\phi_4 + \Phi_7^{(\delta)}\phi_7 + \Phi_8^{(\delta)}\phi_8 + \Phi_9^{(\delta)}\phi_9 + F_\xi^{(\delta)}\left(\frac{\partial\phi}{\partial\xi}\right)_9^{(\delta)} + F_\eta^{(\delta)}\left(\frac{\partial\phi}{\partial\eta}\right)_9^{(\delta)}
\end{aligned} \tag{3.76}$$

Now each quadrant can be treated as an independent element having the size 6 x 6. In the assembly, ϕ is common to all quadrants at the center node whereas all the second derivative terms remain as generalized coordinates, independent of adjacent quadrants. In this approach, although the shock strengths are not directly calculated, the definitions given in (3.53)

enable us to examine the existence of the shocks and their strengths.

3.3.3 Other Approaches

The first finite element applications to transonic flows are those by Chan, Brashears, and Young [35] who employed the least squares in conjunction with the Galerkin approach using cubic triangular elements. No shock boundary treatment was implemented. Chan and Brashears [36] further explored their method to include an unsteady state. Small perturbation theory is utilized in their studies.

Subsequently, Glowinski, Periaux, and Pironneau studied the transonic flow by optimal control [37] of distributed parameter systems, discretized in finite elements. The method of steepest descent was used to solve the system of governing finite element equations.

Wellford and Hafez [38] examined a mixed variational principle for small disturbance transonic flow. The interpolation functions for the velocity potential and the velocity were introduced in the minimization of the mixed variational principle, resulting in two sets of equations, which may be solved iteratively.

Ecer and Akay [39] studied the solution of full potential equation and reported difficulty locating a shock line but the accuracy of the results were otherwise good. In their formulation, the Bateman principle leading to (3.29) was used. The resulting finite element equations are similar to (3.72b) but no shock element formulation (3.52, 3.65, 3.69) was considered in their study.

3.3.4 Unsteady Transonic Flow

For unsteady conditions, we invoke the equation of the form (3.49) and its finite element analog,

$$R_{NM}\ddot{\phi}_M + S_{NM}\dot{\phi}_M - A_{NM}\phi_M = F_N + G_N + S_N \tag{3.77}$$

with

$$R_{NM} = \int_\Omega M_\infty^2 \Phi_N \Phi_M d\Omega$$

$$S_{NM} = \int_\Omega 2M_\infty^2 \ \Phi_N \frac{\partial \Phi_M}{\partial x} \quad \Omega$$

For oscillating airfoil problems, we return to (3.51) with an interpolation field of the form

$$\bar{\phi} = \Phi_N \bar{\phi}_N \tag{3.78}$$

$$\phi_N = \bar{\phi}_{N(R)} + i\bar{\phi}_{N(I)} \tag{3.79}$$

where Φ_N is the interpolation function and $\bar{\phi}_{N(R)}$ and $\bar{\phi}_{N(I)}$ are the real and imaginary parts of the nodal values of $\bar{\phi}$. Substituting (3.78) into (3.51), we obtain two sets of equations similar to (3.77) but one for real part and another for imaginary part. These equations will be solved independently to obtain the nodal values of ϕ from (3.79).

In general, the imposition of boundary conditions for the finite element solutions is simpler than in the finite difference method. In the flight conditions of an airfoil, the exterior boundary is infinite. However, we must use a finite geometry along which the far field analytical solutions [40, 30] may be matched iteratively. On the solid boundary of a body, we require that the velocity normal to the surface be zero; i.e.,

$$V_i n_i = 0$$

or

$$\frac{\partial\phi}{\partial n} = \phi,_i n_i = 0$$

Note also that at infinity, the perturbed velocity is zero,

$$\nabla\phi = \phi,_i = 0$$

The imposition of Dirichlet and Neumann boundary conditions follows the routine procedure.

For unsteady flows, we must satisfy additional boundary conditions, namely, the unsteady Kutter conditions; that is, the pressure across the trailing vortex sheet must be equal.

$$C_p^+ = C_p^- \tag{3.80}$$

where $$C_p = -\frac{2}{U}\left[\frac{\partial\phi}{\partial t} + \frac{\partial\phi}{\partial x_1} + \frac{e}{2U}\left(\frac{\partial\phi}{\partial x_2}\right)^2\right] \tag{3.81}$$

Thus, in terms of potential function, the unsteady Kutter conditions are

$$\left[\frac{\partial\phi}{\partial t} + \frac{\partial\phi}{\partial x_1} + \frac{e}{2U}\left(\frac{\partial\phi}{\partial x_2}\right)^2\right]^+ = \left[\frac{\partial\phi}{\partial t} + \frac{\partial\phi}{\partial x_1} + \frac{e}{2U}\left(\frac{\partial\phi}{\partial x_2}\right)^2\right]^- \tag{3.82}$$

The above conditions must be applied along the upper and lower surfaces of the mean wake position.

If the body is oscillating, then we require that velocity on the surface must be tangent. Let the position of the body geometry at any instant be defined as

$$B(x,y,z,t) = 0 \tag{3.83}$$

Then the surface tangency condition can be satisfied by requiring that the material derivative of the function B with respect to time equal to zero [41].

$$\frac{\partial B}{\partial t} + \frac{\partial B}{\partial x} + \frac{\partial \phi}{\partial x}\frac{\partial B}{\partial x} + \frac{\partial \phi}{\partial y}\frac{\partial B}{\partial y} + \frac{\partial \phi}{\partial z}\frac{\partial B}{\partial z} = 0 \text{ , on } B = 0 \tag{3.84}$$

If the body is thin, we may approximate as

$$\frac{\partial B}{\partial t} + \frac{\partial B}{\partial x} + \frac{\partial \phi}{\partial y}\frac{\partial B}{\partial y} + \frac{\partial \phi}{\partial z}\frac{\partial B}{\partial z} = 0 \tag{3.85}$$

For a two-dimensional flow (z=0), if we let $B(x,y,t) = y - A(x,y,t)$,

$A << 1$, $\frac{\partial A}{\partial y} << 1$,

$$\frac{\partial \phi}{\partial y} = \frac{\partial A}{\partial x} + \frac{\partial A}{\partial t} \tag{3.86}$$

where the function A is taken as

$$A(x,y,t) = ah(x) + bm(x,t) \tag{3.87}$$

with a = airfoil thickness ratio, h(x) = thickness distribution along the axis, b = oscillation amplitude, and m(x,t) = airfoil oscillation function.

In addition to these special boundary conditions (Kutter condition and oscillating body geometry), we must satisfy the standard boundary conditions of Dirichlet and Neumann types in the usual manner.

3.3.5 Example Problems

We consider here a missile consisting of 4 caliber tangent ogive and 9 caliber afterbody, which was studied experimentally in a wind tunnel by Spring [42]. (Fig. 3.5). A typical finite element configuration is shown in Fig. 3.6. Note that the finite elements tangent to the body are installed with two sides constructed normal to the body. If the first layer is made very thin, then the satisfaction of Neumann boundary conditions will be demonstrated by approxomately equal values of velocity potential between the two adjacent nodes in the direction normal to the body.

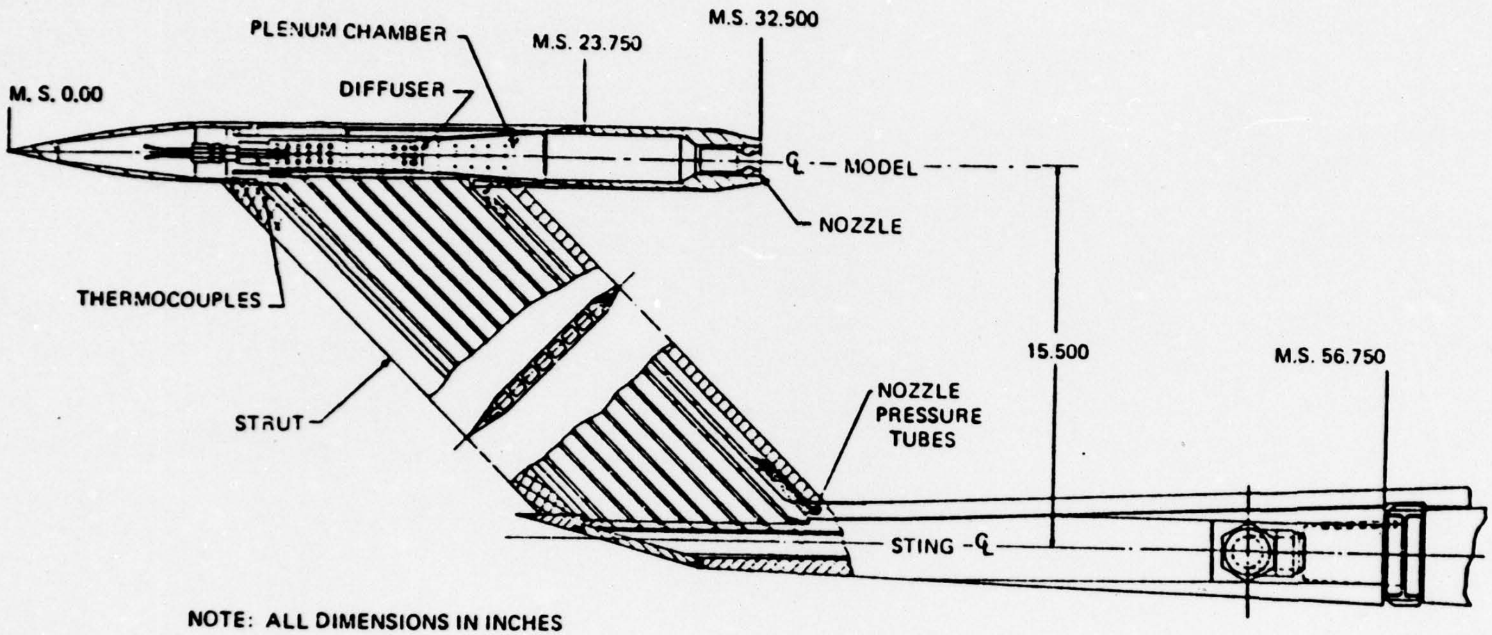

Figure 3.5 Wind Tunnel Test [32]

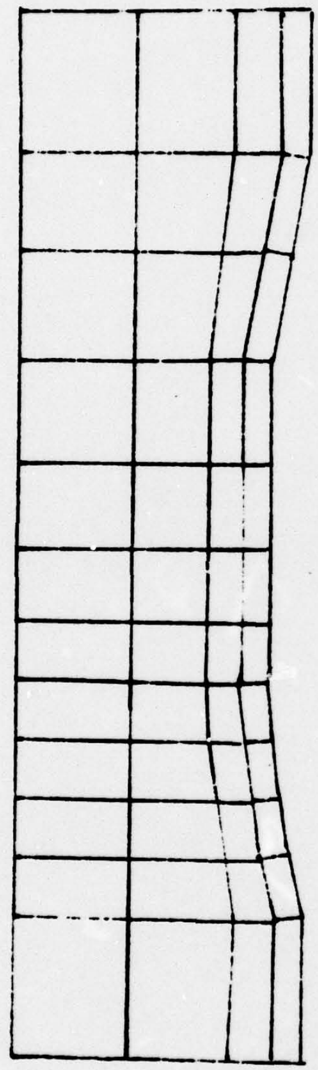

Figure 3.6 Finite Element Model for Wind Tunnel Test [32]

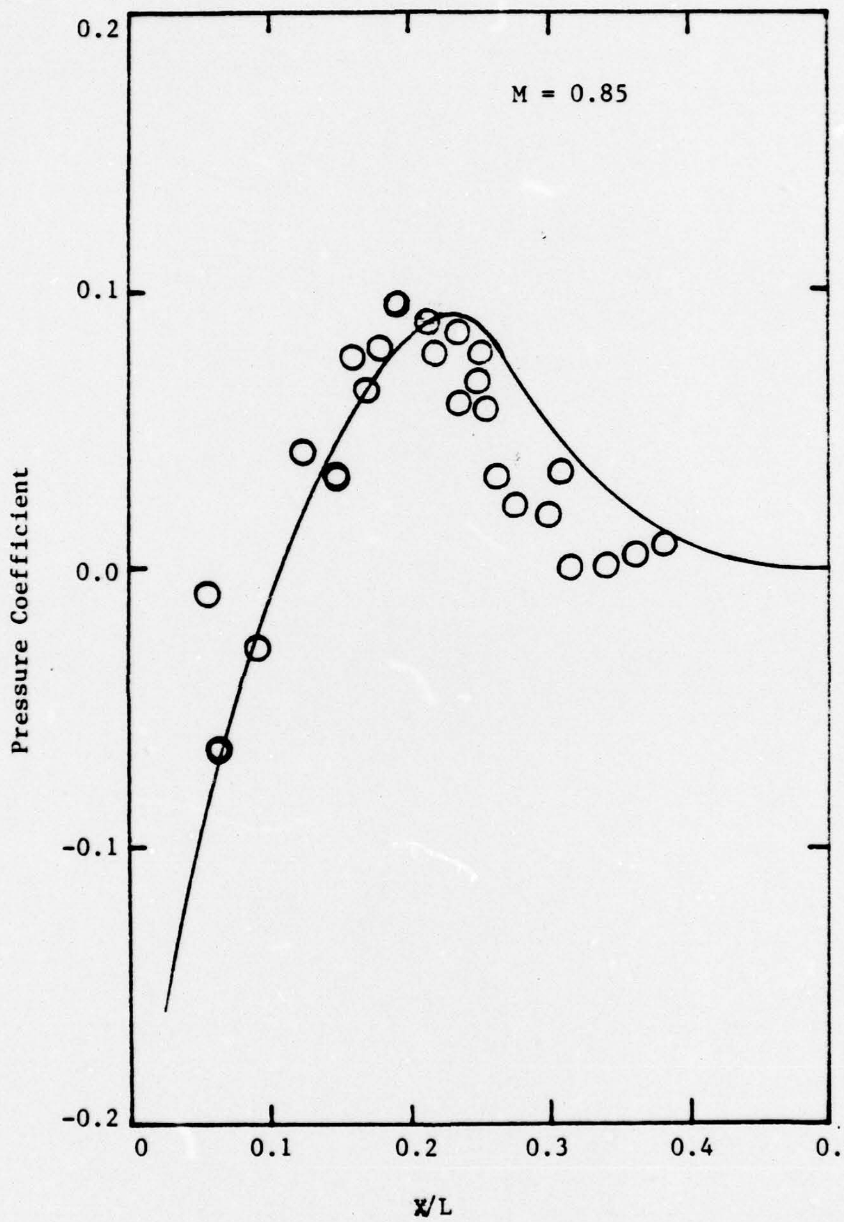

Figure 3.7a Pressure Coefficients for the Problem in Fig. 3.6, circles indicate the experimental results [42], M = 0.85

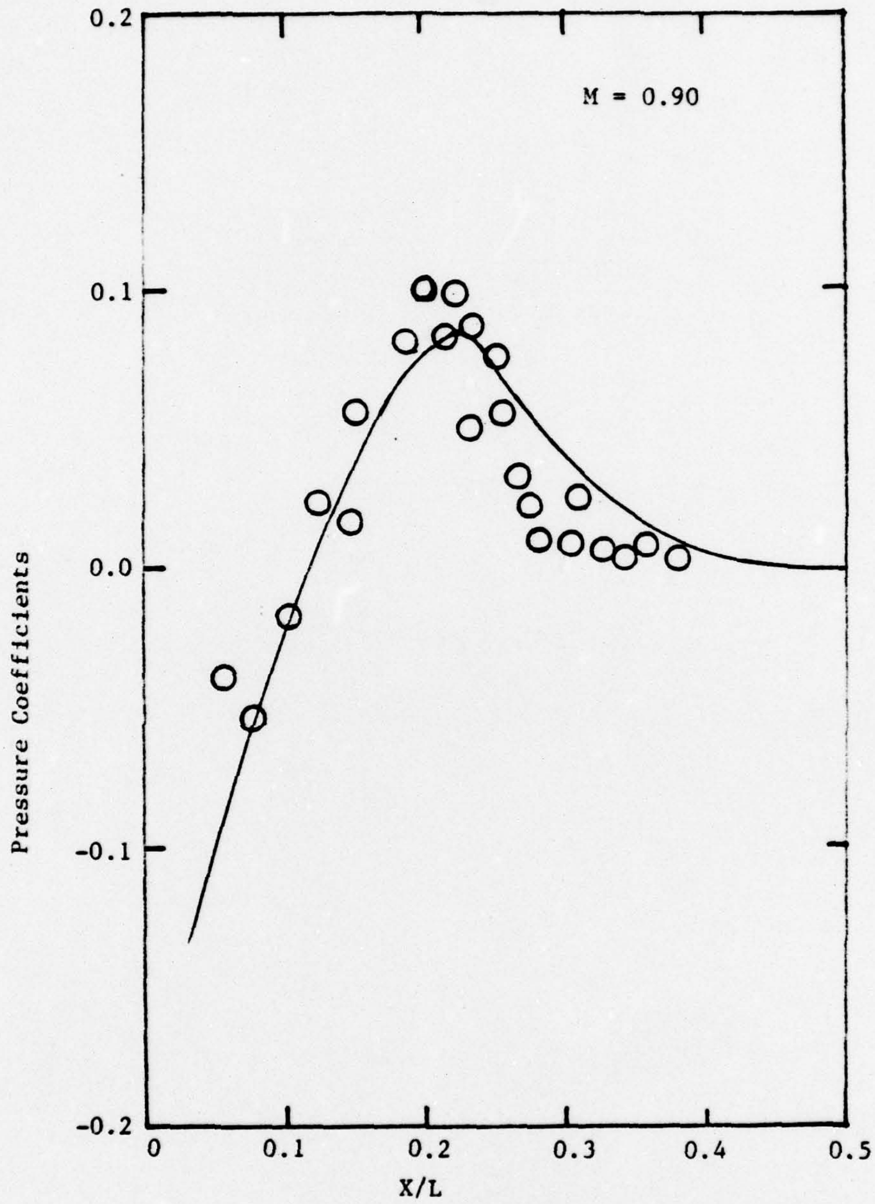

Figure 3.7b Pressure Coefficients for the problem in Fig. 3.6, circles indicate the experimental results, [42], M = 0.9

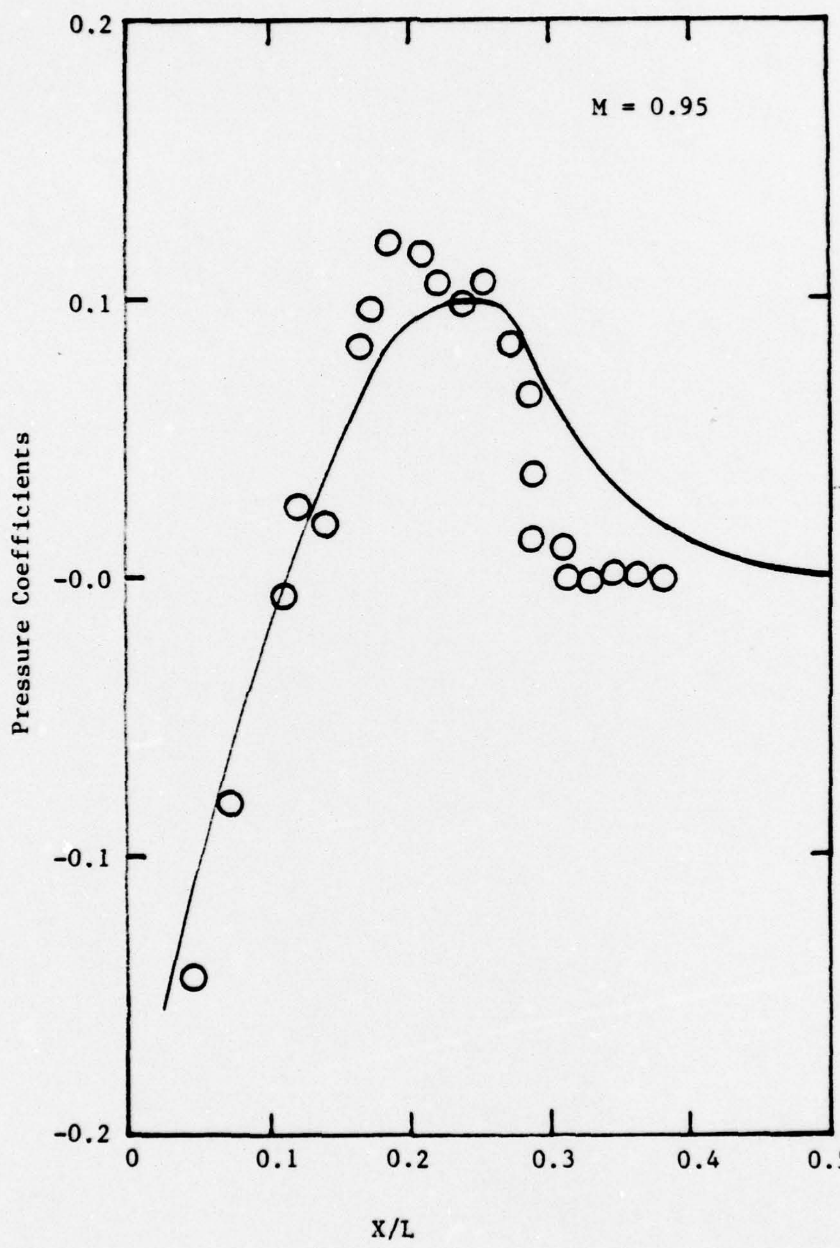

Fig. 3.7c Pressure coefficients for the problem in Fig. 3.6, circles indicate the experimental results [42], M = 0.95

The solution based on discontinuous functions (3.52) together with the global finite elements equations (3.69) is obtained through the iterative process (3.71). It should be noted that less computer time is expended if the functions (3.76) are used. This is due to simpler integration ranging from -1 to 1 instead of half-ranges required in (3.62). Both integration schemes appear to yield identical results.

The pressure coefficients for M = 0.85, 0.90, 0.95 are plotted in Figure 3.7. Slight deviations between the experimental results and finite element calculations are assumed to be due to the far-field boundary conditions of finite element model being simulated by porous wall of experiments, as well as other possible factors involved in both computational and experimental procedures.

Note that for small perturbation, the expression $Y_i^{(n)}$ will assume a simplified form (3.54) with all other procedures remaining the same.

3.3.6 Error Estimates

The mathematical error estimates on mixed equations have received growing attention in recent years. For simplicity we may consider the mixed equation of the type

$$\frac{\partial}{\partial x}\left[Q(x,y)\,\frac{\partial u}{\partial x}\right] + \frac{\partial^2 u}{\partial y^2} = f \quad \text{in } \Omega \tag{3.88}$$

where Q changes sign in Ω. Futher simplification leads to the Tricomi problem

$$y\,\frac{\partial^2 u}{\partial x^2} + \frac{\partial^2 u}{\partial y^2} = f \tag{3.89}$$

Trangenstein [43] examines Tricomi equation and obtains satisfactory error estimates on the elliptic region although the solution on the parabolic line $y = 0$ and in hyperbolic region $y < 0$ suffers difficulty.

Subsequently Aziz and Leventhal [44] studied the first order system

$$Lu = A_1\frac{\partial u}{\partial x} + A_2\frac{\partial u}{\partial y} + A_3 u = f \text{ in } \Omega \tag{3.90}$$

$$Bu = 0 \qquad\qquad \text{on } \Gamma \tag{3.91}$$

where L is symmetric positive and B is admissible [45]. Let V_h be a finite dimensional subspace of $H^1(\Omega)$ where h denotes a mesh parameter such that $U_h \varepsilon V_h$ and $\Psi_h \varepsilon V_h$. Let the finite element equation be constructed from (3.90) and (3.91) to find $U_h \varepsilon V_h$ such that

$$(LU_h,\Psi_h)_{L_2(\Omega)} + (NU_h,\Psi_h)_{L_2(\Omega)} = (f,\Psi_h)_{L_2(\Omega)}, \quad \forall \ \Psi_h \varepsilon V_h \tag{3.92}$$

where $U_h = \Phi_i U_i$ and $\Psi_h = \Psi_i U_i$. This leads to the linear system

$$A_{ij}U_j = F_i \tag{3.93}$$

with

$$A_{ij} = (L\Phi_i,\Psi_j)_{L_2(\Omega)} + (N\Phi_i,\Psi_j)_{L_2(\Omega)}$$

$$F_i = (f,\Psi_i)$$

It can easily be shown [46] that

$$\|U_h\|_{L_2(\Omega)} \leq c\|f\|_{L_2(\Omega)} \qquad c > 0 \tag{3.94}$$

Now let the subspaces V_h be restricted to functions U_h of degree less than or equal to k. If the solution u in (3.90) and (3.91) are in $H^{k+1}(\Omega) \cap C^o(\Omega)$, then we obtain [46]

$$\| u-U_h\|_{L_2(\Omega)} = O(h^k) \tag{3.95}$$

This is contrary to the results numerically obtained [44] for the Tricomi problem. A similar conclusion arises in the least squares approximation.

Consider the first order system

$$\frac{\partial u}{\partial y} = f(x), \qquad 0 < x,y < 1$$

$$u(x,0) = 0, \qquad 0 < x < 1$$

It can be shown [47] that, away from the boundaries $x = 0$ and $x = 1$, the error is $O(h^2)$ while near $x = 0$ or $x = 1$ it is $O(h)$. The overall L_2 error is

$$\left\{\iint |u-u_h|^2\right\}^{1/2} = O(h^{3/2})$$

one half less than optimal, but better than the $O(h)$ predicted by LeSaint [46].

The theoretical error estimates for the full nonlinear potential equation are not available at this time. However, our numerical results indicate somewhere between $O(h\ )$ and $O(h^k)$ pointwise for the problems formulated for the discontinuous functions described earlier. This error analysis is for the potential function; the rates of convergence for the velocities calculated from the potential functions are, in general half as low.

Let us now investigate the rates of convergence for the problem of Fig. 3.6. Upon various discretizations, calculations are carried out to determine the slopes of the pointwise errors at x=10 on the airfoil surface. The results for $M = 0.9$ are presented in Fig. 3.8. It is seen that the rates of convergence for the full potential equation and small perturbations are $O(h^{1.05})$ and $O(h^{1.13})$.

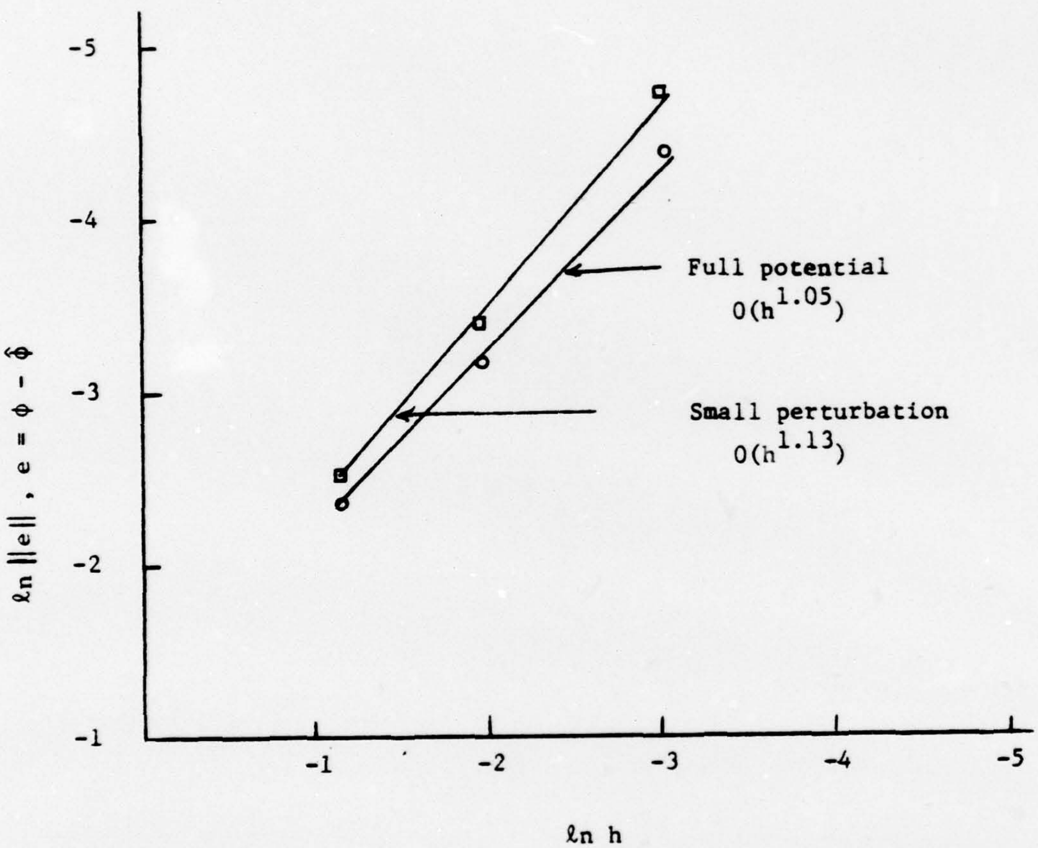

Figure 3.8 Pointwise Error at x = 10 on the Airfoil Surface, M = 0.9

3.3.7 Remarks

It has been observed that the Galerkin Method tends to be unstable for M > 0.95, although stability and accuracy may be restored if prohibitively large number of elements are used. Only, recently, the author has investigated the optimal control penalty least square finite elements. Following the initial success of this method in convective heat transfer problems [17] we began exploration into the Tricomi equation and the small perturbation equation [15]. In the following section we present the details of the optimal control penalty least square finite elements.

4. OPTIMAL CONTROL PENALTY LEAST-SQUARE FINITE ELEMENTS

4.1 General

We consider the optimal control problems of the type

$$\min_{\phi\epsilon\Phi} \int_{\Omega} [\nabla^2\phi + G]^2 \, d\Omega \tag{4.1}$$

where Φ is a space of admissible functicns, a suitable choice for Φ being the space $H_0^1(\Omega)$. An alternative form of (4.1) may be constructed by constraints

$$u = \frac{\partial\phi}{\partial x} \tag{4.2}$$

$$v = \frac{\partial\phi}{\partial y} \tag{4.3}$$

such that

$$\min_{\phi\epsilon\Phi} \int_{\Omega} \left\{ \left[\frac{\partial u}{\partial x} + \frac{\partial v}{\partial y} + G\right]^2 + \lambda\left(u - \frac{\partial\phi}{\partial x}\right)^2 + \mu\left(v - \frac{\partial\phi}{\partial y}\right)^2 \right\} d\Omega \tag{4.4}$$

Here λ and μ are the penalty constants. It is seen that the expression given by (4.4) represents the first order system of integrodifferential equation and leads to a symmetric, positive-definite system of finite element equations. The advantage of such formulation is its ability to provide type-independent solutions.

The terms of G for Tricomi equation, small perturbation equation, and full potential equation are expressed as follows:

Tricomi:

$$G = -\alpha\frac{\partial u}{\partial x}, \quad \alpha = 1 - y \tag{4.5}$$

Small perturbation:

$$G = -M_\infty^2 \frac{\partial u}{\partial x}\left(\frac{u(1+\gamma)}{U_\infty} + 1\right) \quad . \tag{4.6}$$

Full potential equation:

$$G = \frac{1}{a^2}\left(u^2 \frac{\partial u}{\partial x} + v^2 \frac{\partial v}{\partial y} + 2uv \frac{\partial u}{\partial y}\right) \tag{4.7}$$

The advantage of the present formulation is attributed to the first order system of integrodifferential equation and to the possibility of using linear trial functions. Thus we write

$$\phi = \Phi_\alpha \phi_\alpha, \; u = \Phi_\alpha u_\alpha, \; v = \Phi_\alpha v_\alpha \tag{4.8}$$

where α denotes the global node.

The operation required in (4.4) takes the form

$$\delta J = \frac{\partial J}{\partial \phi_\alpha} \delta\phi_\alpha + \frac{\delta J}{\partial u_\alpha} \delta u_\alpha + \frac{\partial J}{\partial v_\alpha} \delta v_\alpha = 0 \tag{4.9}$$

where J represents the integral in (4.4). Substituting (4.8) in (4.9) and setting each of the derivatives on the right hand side equal to zero, we obtain

$$\begin{bmatrix} A_{\alpha\beta} & B_{\alpha\beta} & C_{\alpha\beta} \\ B_{\beta\alpha} & D_{\alpha\beta} & E_{\alpha\beta} \\ C_{\beta\alpha} & E_{\beta\alpha} & F_{\alpha\beta} \end{bmatrix} \begin{bmatrix} u_\beta \\ v_\beta \\ \phi_\beta \end{bmatrix} = \begin{bmatrix} G_\alpha \\ H_\alpha \\ I_\alpha \end{bmatrix} \tag{4.10}$$

Note that the coefficient matrix in (4.10) is symmetric and positive-definite, which leads to the decisive role ensuring the stability and convergence as the resulting equations are type-insensitive.

4.2 Solution Procedure

Although compact in form as seen in (4.10) the matrix on the left hand side is nonlinear. The solution is carried out using the Newton-Raphson procedure together with conjugate gradient and steepest descent. Let us

consider the nonlinear equations resulting from (4.10) in the form

$$K_{ij}X_j - F_i = R_i \tag{4.11}$$

where i,j denote the total number of equations. The standard Newton-Raphson iterative process may be recast in the form

$$J_{ij}^{(n)}\, X_j^{(n+1)} = J_{ij}^{(n)}\, X_j^{(n)} - R_i^{(n)} = B_i^{(n)} \qquad (.12)$$

where $B_i^{(n)}$ is defined as

$$B_i^{(n)} = J_{ij}^{(n)}\, X_j^{(n)} - K_{ij}^{(n)}\, X_j^{(n)} - F_i^{(n)} \tag{4.13}$$

and

$$J_{ij}^{(n)} = \frac{\partial R_i^{(n)}}{\partial X_j} \tag{4.14}$$

It is convenient to calculate the Jacobian for each element and assemble into the global form. The solution implied in (4.12) may begin with the conjugate gradient method as follows:

Let

$$V_i^{(1)} = F_i^{(0)} - K_{ij}X_j^{(0)} = F_i^{(0)}$$

Then

$$\alpha^{(1)} = V_iV_i \;/\; V_iK_{ij}V_j = V_ir_i \;/\; V_iA_{ij}V_j$$

$$X_i^{(2)} = X_i^{(1)} + \alpha^{(1)}V_i^{(1)}$$

$$r_i^{(n+1)} = r_i^{(n)} - \alpha^{(n)}A_{ij}V_j^{(n)}$$

$$\beta^{(n)} = -\, K_{ij}V_ir_j^{(n+1)}$$

$$V_i^{(n+1)} = r_i^{(n+1)} + \beta^{(n)}V_i^{(n)} \tag{4.15}$$

This iterative procedure continues until the residual $r_i \leq 10^{-7}$. The values from this method are used as the first estimates of $X_j^{(n)}$'s in (4.12).

In order to solve (4.12), the method of steepest descent is used between each cycle of Newton-Raphson iterations. It has been observed that the steepest descent is more efficient than the conjugate gradient in stabilizing and inducing a rapid convergence for the Newton-Raphson iterations. The steepest descent equations are

$$X_k^{(n+1)} = X_k^{(n)} + (r_i^{(n)} r_i^{(n)} / \, r_i^{(n)} J_{ij}^{(n)} r_j) r_k^{(n)} \qquad (4.16)$$

where

$$r_i^{(n)} = B_i^{(n)} - J_{ij}^{(n)} X_j^{(n)}$$

In general, approximately 10 cycles of Newton-Raphson iterations are required for satisfactory convergence. The flow diagram shown in Table 4.1 outlines the basic steps in the proposed solution procedure.

The treatment of shock elements can be handled similarly as in Section 3. However, the generalized coordinates Q_α in (4.64) are replaced by X_α and the jump condition (shock boundary condition) equivalent to (4.66) is written as

$$\lambda_k q_{k\alpha} X_\alpha = 0 \qquad (4.17)$$

These observations lead to

$$\begin{bmatrix} K_{\alpha\beta} & q_{k\alpha} \\ q_{k\beta} & 0 \end{bmatrix} \begin{bmatrix} X_\beta \\ \lambda_k \end{bmatrix} = \begin{bmatrix} F_\alpha \\ 0 \end{bmatrix} \qquad (4.18)$$

Note that the new generalized coordinates X_β contain the values of derivatives of velocity potential but not the differences of these values between two adjacent quadrants of an element. However, the shock element can be defined as the iterative solution converges.

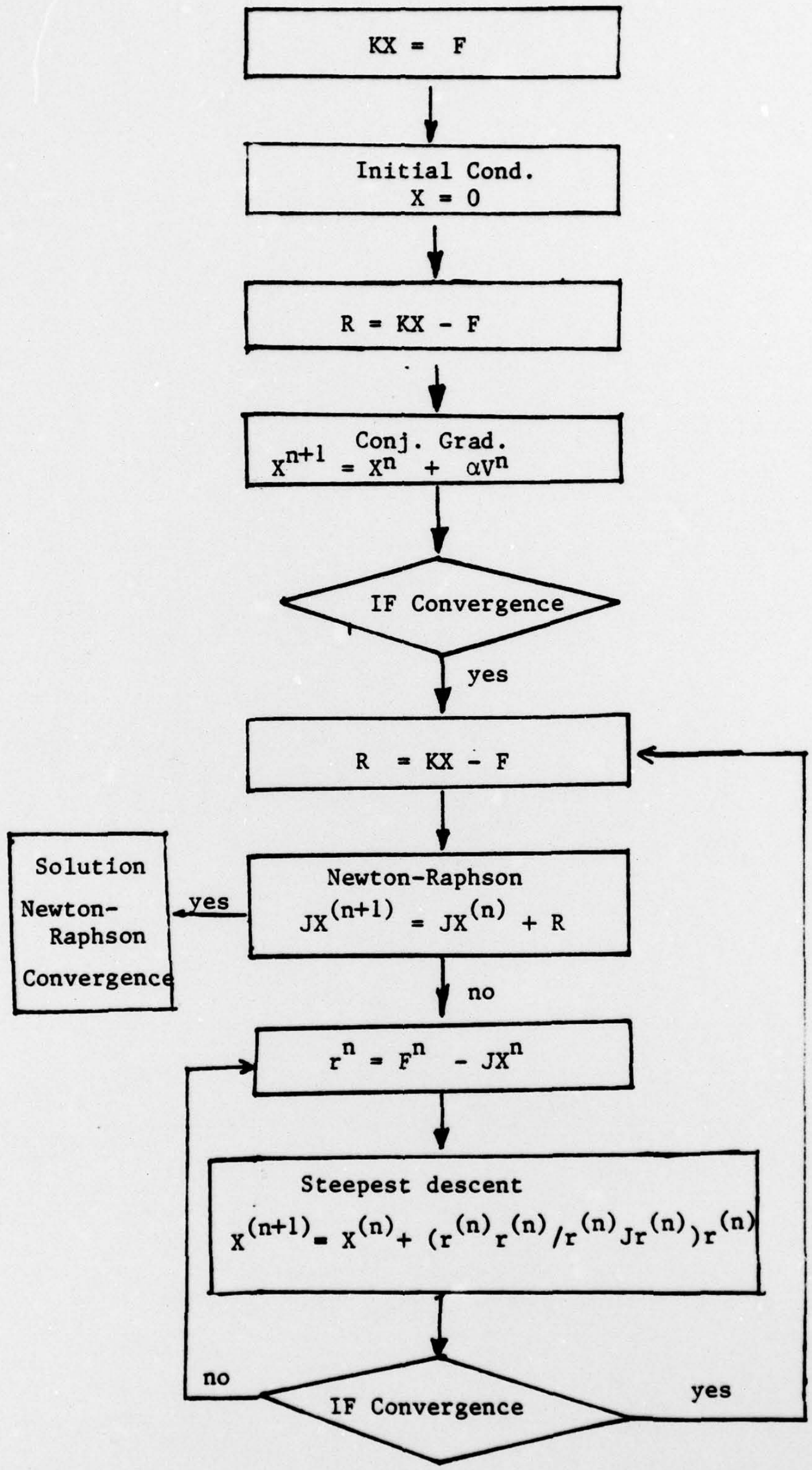

Table 4.1 Flow Diagram for Solution Procedure

4.3 Examples

4.3.1 Tricomi

We consider the solution of Tricomi equation in the form

$$\phi = x^4 y - x^2 y^4 + \frac{y^7}{21} \tag{4.19}$$

$$u = 4x^3 y - 2xy^4$$

$$v = x^4 - 4x^2 y^3 + \frac{y^6}{6}$$

which satisfies

$$y \frac{\partial^2 \phi}{\partial x^2} + \frac{\partial^2 \phi}{\partial y^2} = 0 \qquad 0 \le x \le 1$$

or

$$y \frac{\partial u}{\partial x} + \frac{\partial v}{\partial y} = 0 \qquad 0 \le x \le 1$$

We let the penalty constants $\lambda = \mu$ to vary between small and large values and determine the optimum magnitude. As seen in Fig. 4.1, $\lambda = 1.383$ appears to be optimum. Note that the comparison with exact solution is quite satisfactory as seen in Fig. 4.2. The rate of convergence with respect to mesh size is plotted in Fig. 4.3, which gives approximately $O(h)$.

For $y \le 0$ the Galerkin method or the standard finite difference method fails miserably. The present approach as given by (4.1) overcomes the type-dependency of the solution and achieves an excellent stability and accuracy as the scheme provides a type-independent property, symmetric and positive-definite matrix. The accuracy achieved from the present technique has been shown to be far superior to other reported results [44].

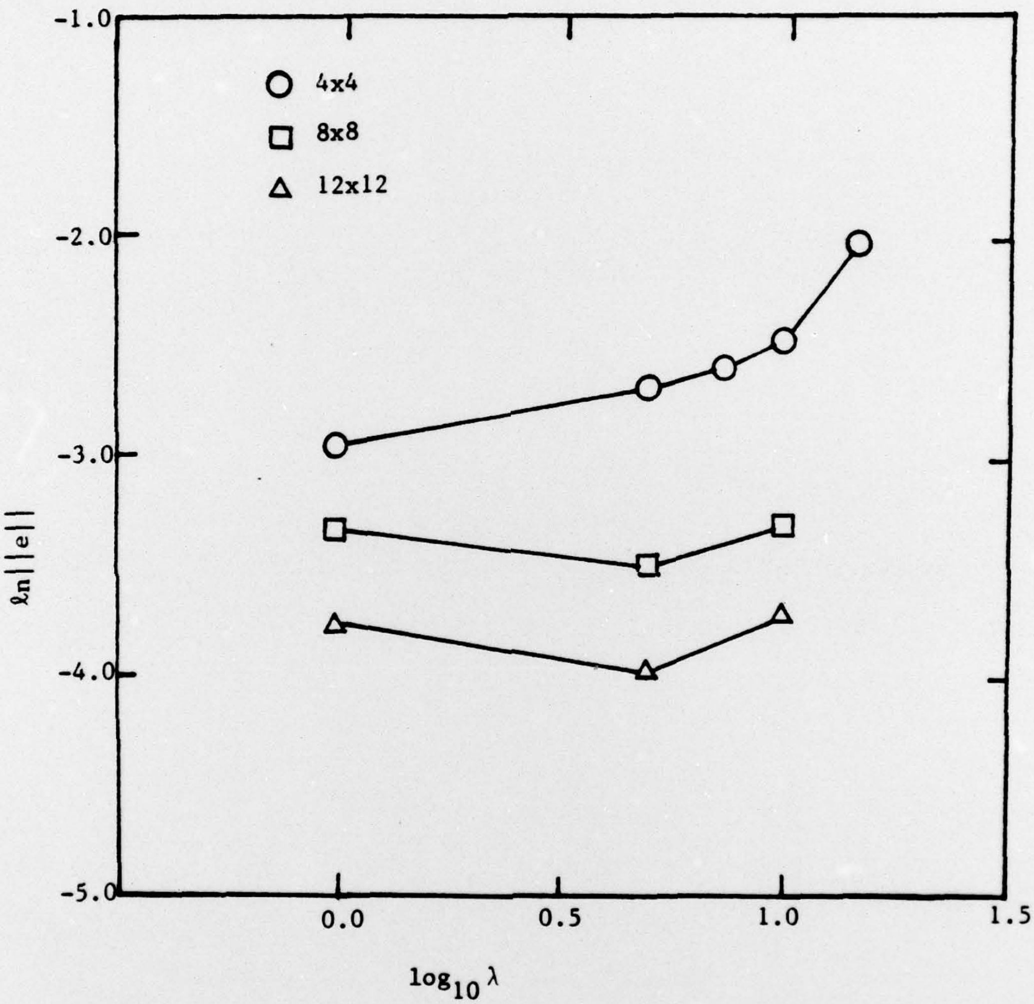

Figure 4.1 Error vs Penalty constants for mesh sizes 4x4, 8x8, 12x12, solution of Tricomi equation, Dirichlet Boundary Conditions, $\phi = x^4y - x^2y^4 + y^7/21$.

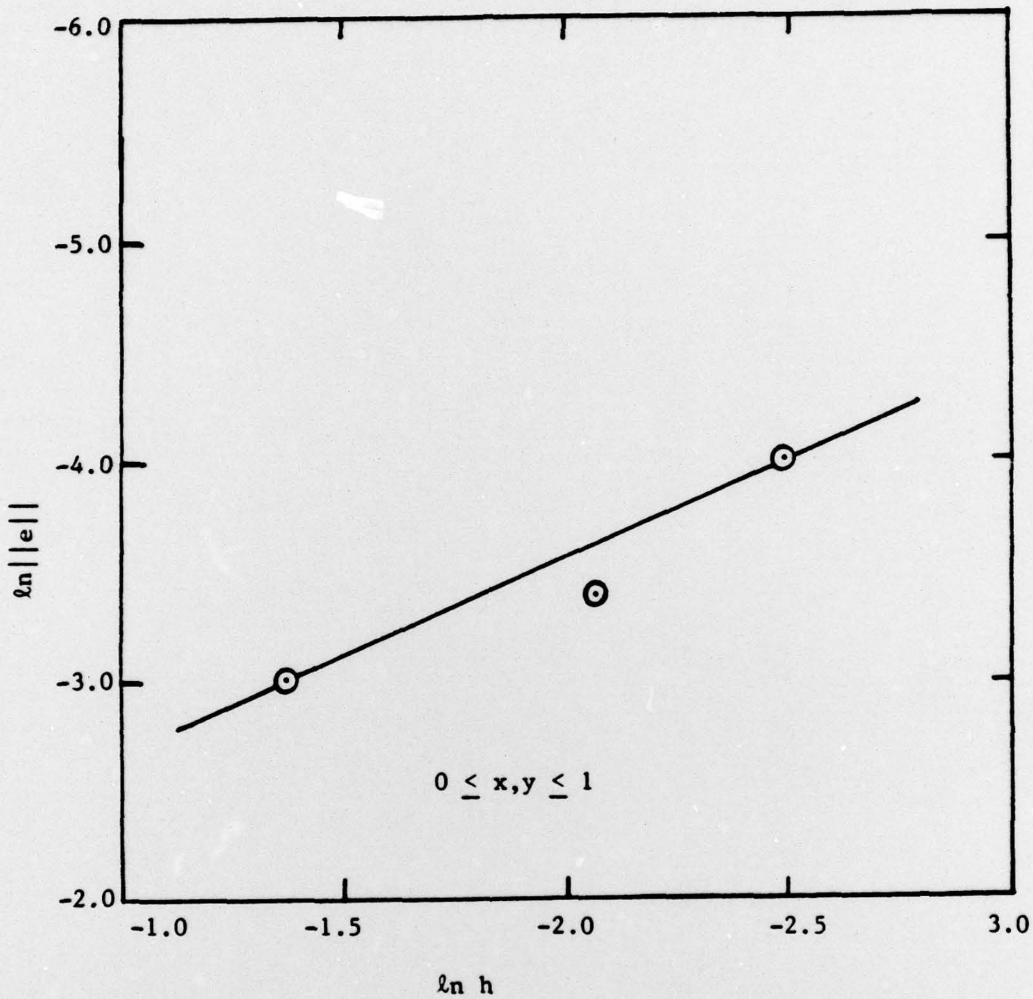

Figure 4.2 Error vs Mesh size at optimal penalty constant, solution of Tricomi equation, $\phi = x^4y - x^2y^4 + y^7/24$.

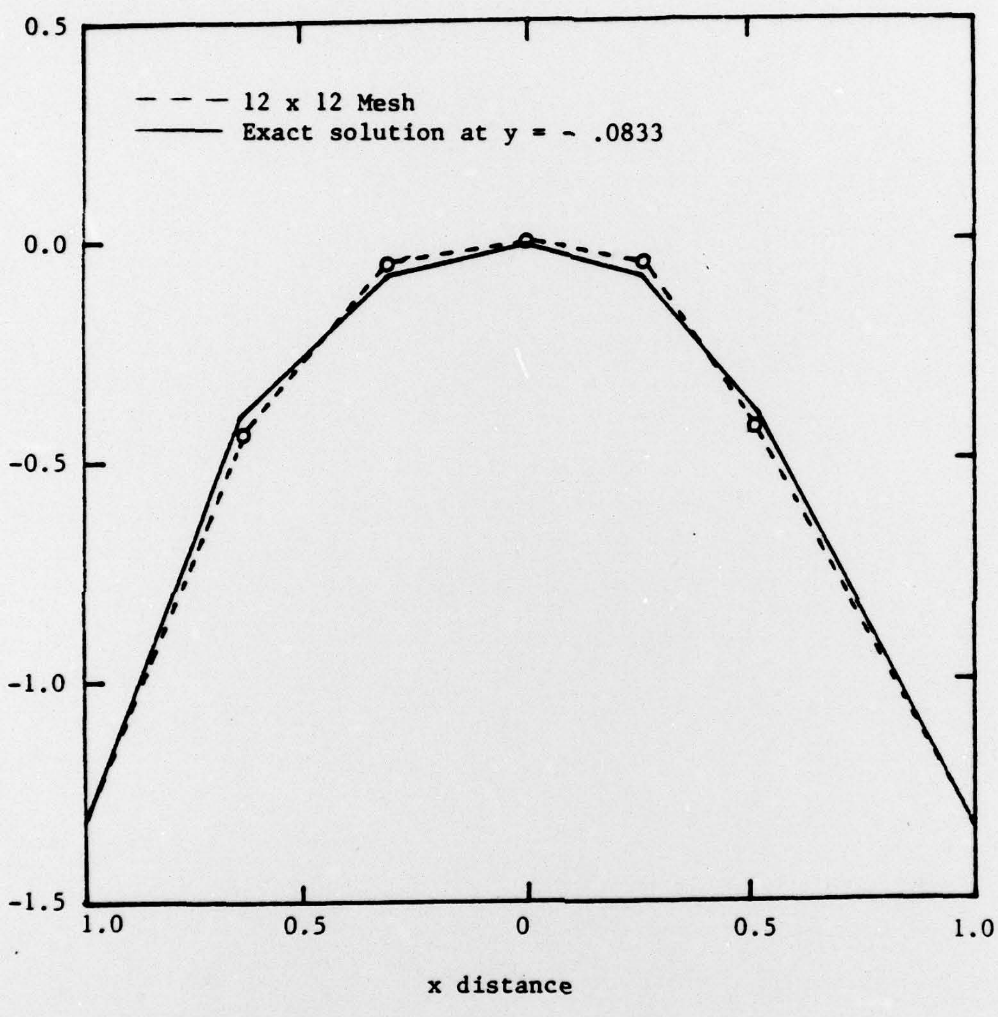

Figure 4.3 Solution of Tricomi equation, comparison of ϕ with exact solution, $\phi = x^4y - x^2y + y^7/21$.

4.3.2 Transonic Equations

Consider the cost function of the form

$$J = \int_\Omega \left[\left(\frac{\partial u}{\partial x} - \frac{\partial v}{\partial y} - G - g(x,y) \right)^2 + \lambda \left(u - \frac{\partial \phi}{\partial x} \right)^2 + \mu \left(v - \frac{\partial \phi}{\partial y} \right)^2 \right] d\Omega \tag{4.20}$$

where G is given by (4.6) or (4.7). For small perturbation flow we define

$$g(x,y) = -(1-M_\infty^2)(1-y)(2y-2x)(1-x) + 2x(1-x) + + 2M_\infty^2 \frac{(1+\gamma)}{U_\infty} \left[-(1-y)xy + (1-x)(1-y)y \right] \left[y(1-y) \right] \tag{4.21}$$

The exact solution assumes the form

$$\phi = (1-x)(1-y)xy \tag{4.22}$$

The optimum penalty constants ($\lambda = \mu$) can be seen in Fig. 4.4 and the finite element solutions are shown in Fig. 4.5. The rates of convergence for various variables are plotted in Fig. 4.6. The stability and accuracy along with the rate of convergence achieved in this method are superior to any previous approaches which have been reported to date.

With conviction that the optimal control penalty least squares finite elements are capable of obtaining type-independent solutions in transonic flows as tested with exact solutions, the procedure for shock elements and discontinuous solution can be combined.

The main body of this report concerns the Galerkin approach as proposed in the original contract [48,49]. The optimal control penalty finite element method is a new idea which has grown out of the present research. This new approach warrants extensive further research as the author is convinced that the problems of discontinuity and exact behavior of shock waves can be most effectively studied by the optimal control penalty finite element method.

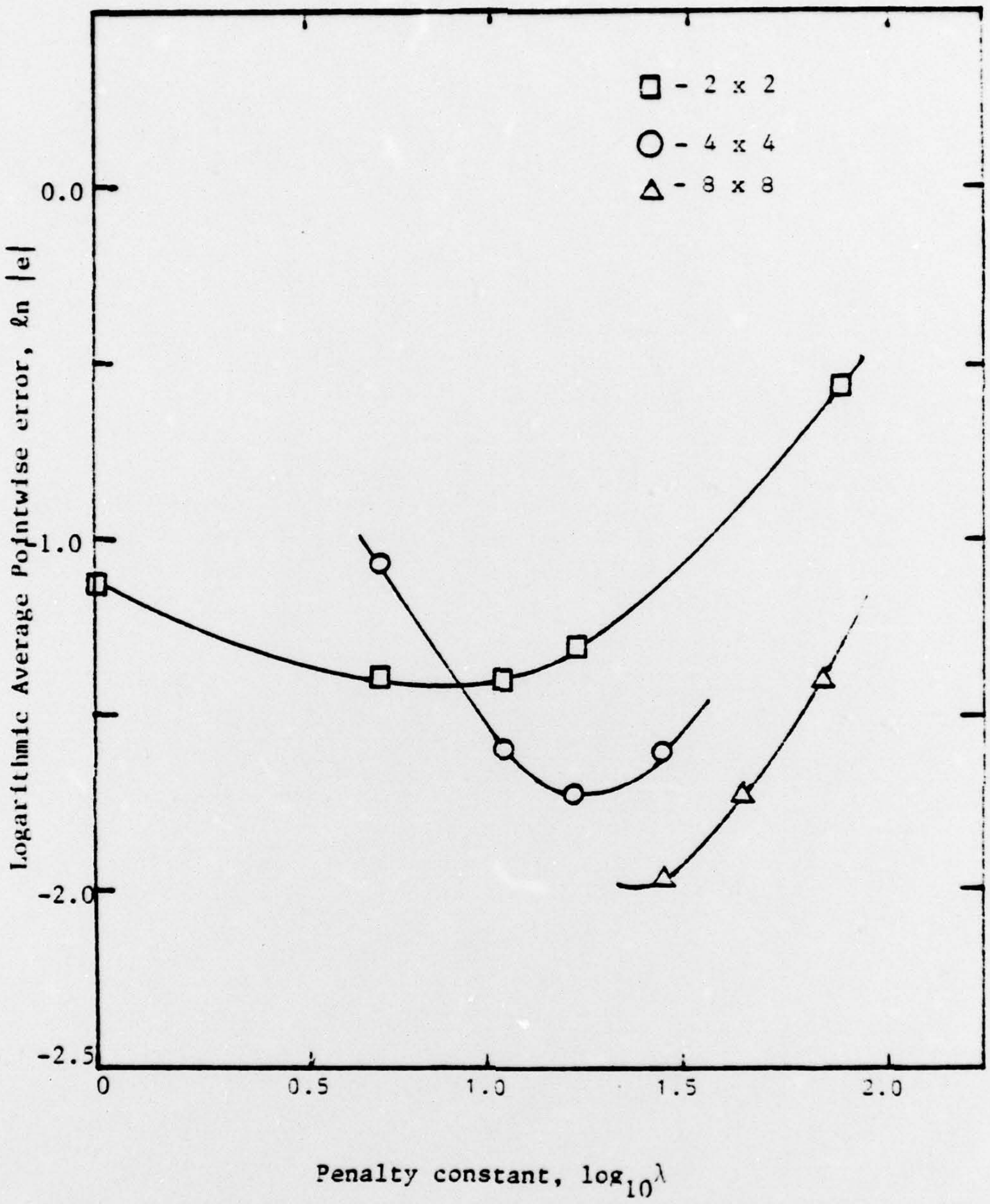

Fig. 4.4 Small perturbation transonic equation- Logarithmic average pointwise error vs penalty constants. $\phi = (1-x)(1-y)xy$

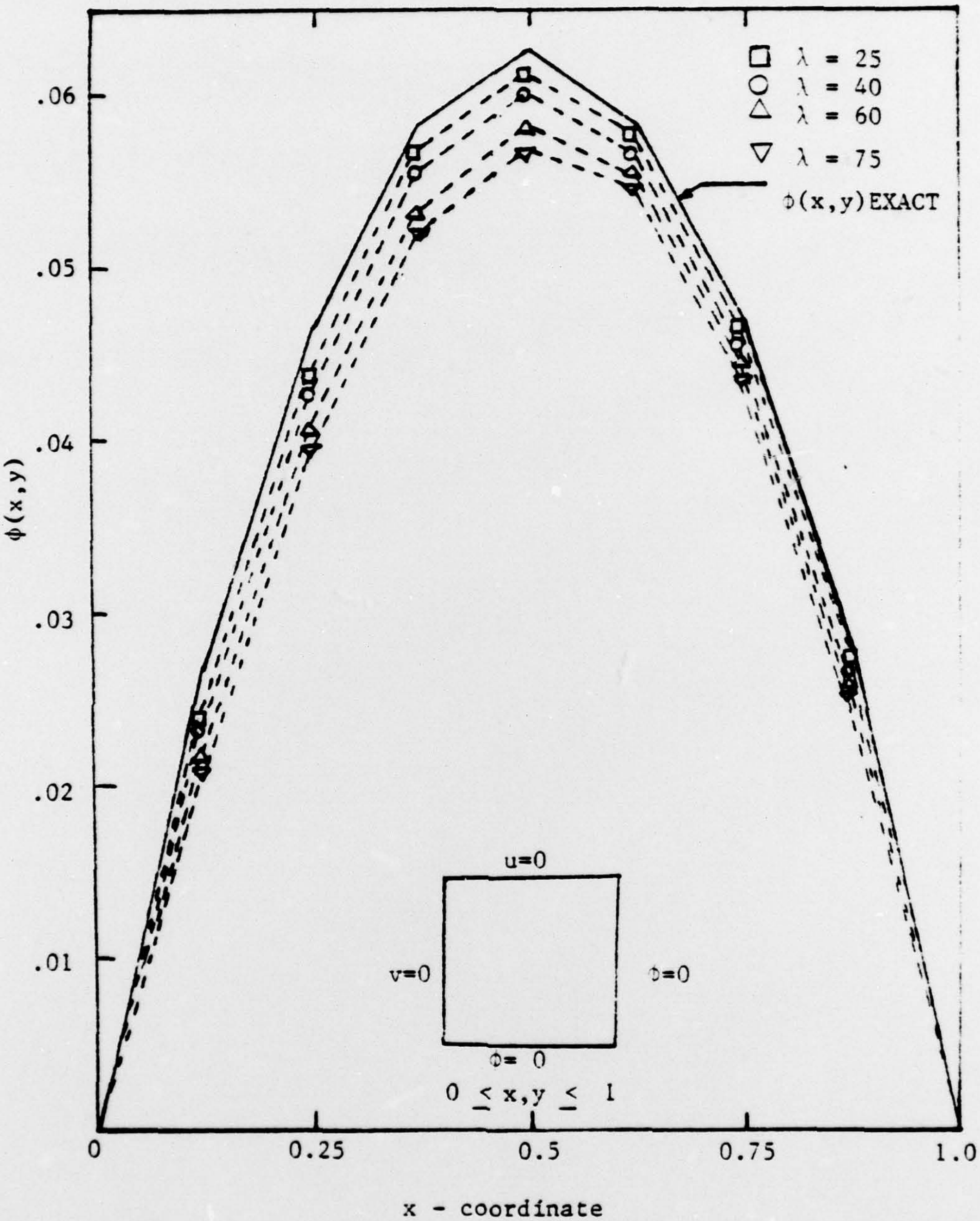

Fig. 4.5 Small perturbation transonic equation-Comparison with exact solution, $y=0.5$, 8×8 mesh, $\phi = (1-x)(1-y)xy$

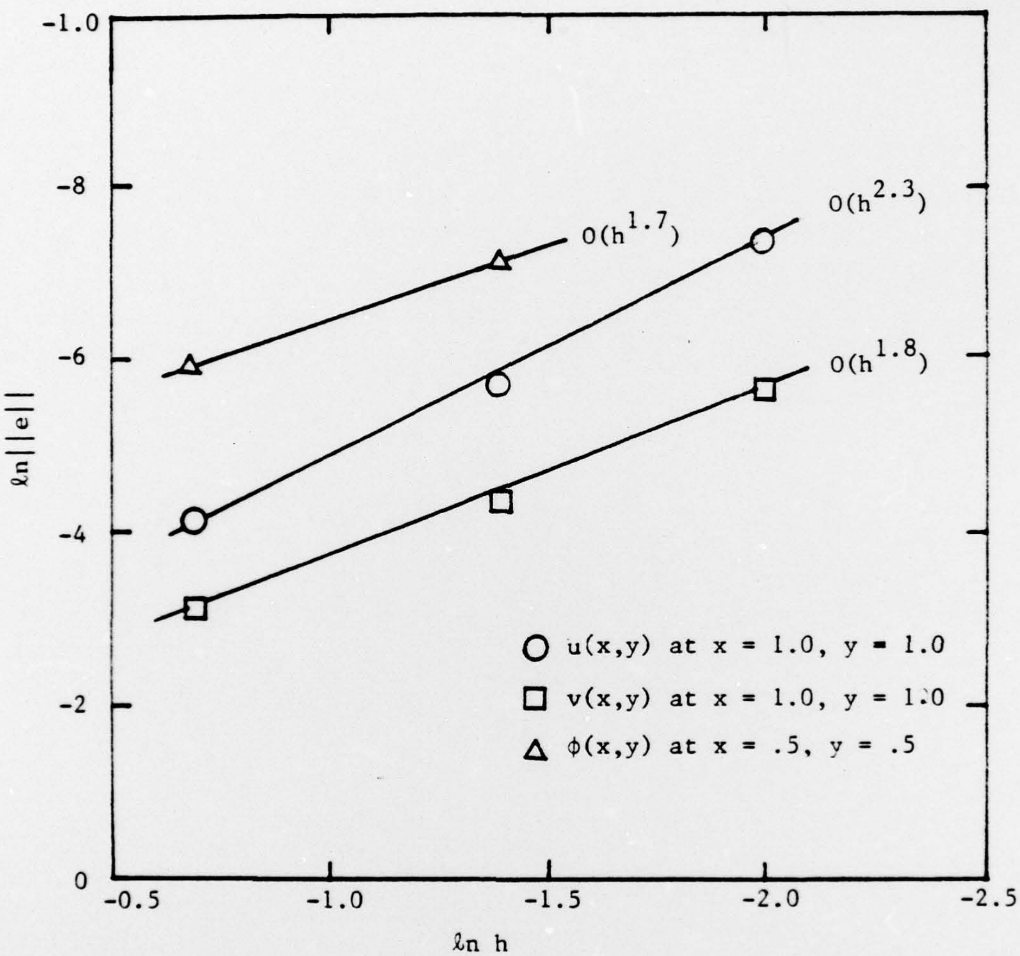

Figure 4.6 Pointwise error rate of convergence for small perturbation equation, $\lambda = 10$ for 2 x 2 mesh $\lambda = 50$ for 8 x 8 mesh, $\phi = (1-x)(1-y)xy$

5. CONCLUSIONS AND RECOMMENDATIONS

The work carried out herein represents the Galerkin finite element method for solving aerodynamics problems with emphasis on transonic flows. A shock element concept was proposed and computations have been carried out. In this process, a quadratic isoparametric element is divided into quadrants with each quadrant having independent trial functions. This idea allows discontinuities at the center of an element and shocks are allowed to develop freely. Rankin-Hugoniot conditions are satisfied accurately.

Although this method is efficient until freestream Mach number reaches approximately 0.95, the solution seems to deteriorate significantly for $M > 0.95$. Toward the end of this contract research period, the author proposed a new approach-optimal control penalty finite elements. This method is suited ideally for problems of discontinuity and shock waves as a consequence of changes in the type of partial differential equations. The resulting equations are symmetric and positive-definite, their solution being type-independent. Numerous examples indicate that both stability and accuracy are maintained very satisfactorily for Tricomi and small perturbation equations. Detailed calculations applied to the full potential equations using this approach are beyond the scope of the present study.

In summary and in retrospect, the finite element method, although extremely successful in elliptic boundary value problems, has just begun in aerodynamics. In due time, its versatility is expected to be demonstrated in some of the most difficult problems in aerodynamics. It appears to this author that a full exploration of the optimal control penalty finite elements should be launched since this report has proved its potential.

REFERENCES

1. Babuska, I. and Aziz, A. K., "Lectures on the Mathematical Foundations of the Finite Element Method," Mathematical Foundations of the Finite Element Method with Applications to Partial Differential Equations, A. K. Aziz (Ed), Academic Press, New York, 1972, pp. 1-345.

2. Ciarlet, P. G. and Raviart, P. A., "General Lagrange and Hermit Interpolation in R^n with Applications to the Finite Element Method," Arch. Mech. Anal., Vol. 46, 1972, pp. 177-199.

3. Strang, G. and Fix, G., "An Analysis of the Finite Element Method," Prentice Hall, Englewood Cliffs, N.J., 1972.

4. Oden, J. T. and Reddy, J. N., "Introduction to Mathematical Theory of Finite Elements," Wiley Interscience, New York, 1976.

5. Ciarlet, P. G., "Finite Element Method for Elliptic Problems," North-Holland Publishing Co., 1978.

6. Finite Elements in Fluids I, II, III, Oden, J. T., Gallagher, R. H., Taylor, C., and Zienkiewicz (Ed), John Wiley and Sons, New York, 1975, 1978.

7. Chung, T. J., "Finite Element Analysis in Fluid Dynamics," McGraw-Hill Book Co., New York, 1978.

8. Chung, T. J., "Recent Advances in Transonics with Finite Elements," Proc. U.S. Japan Seminar on Interdisciplinary Finite Element Analysis, Cornell University, Aug. 7-11, 1978.

9. Christie, I., Griffiths, D. F., Mitchell, A. R., and Zienkiewicz, O. C., "Finite Element Methods for Second Order Differential Equations with Significant First Order Derivatives," Int. J. Num. Meth. Engng., Vol. 10, 1976, pp. 1389-1396.

10. Heinrich, J. C., Huyakorn, P. S., Zienkiewicz, O. C., and Mitchell, A. R., "An Upwind Finite Element Scheme for Two-Dimensional Convective Transport Equation," Int. J. Num. Meth. Engng., Vol. 11, No. 1, 1977, pp. 131-144.

11. Christie, I. and Mitchell,A. R., "Upwinding of High Order Galerkin Methods in Conduction-Convection Problems," Int. J. Num. Meth. Engng., Vol. 12, 1978, pp. 1764-1771.

12. Hughes, T. J. R. and Brooks, A., "A Multi-Dimensional Upwind Scheme with No Crosswind Diffusion," Proc. Symposium on Finite Element Methods for Convection Dominated Flows, ASME Winter Annual Meeting, New York, Dec. 3-7, 1979.

13. Gartling, D. K., "Some Comments on the Paper by Heinrich, Huyakorn, Zienkiewicz, and Mitchell," Int. J. Num. Meth. Engng., Vol. 12, 1978, pp. 187-190.

14. Gresho, P. M. and Lee, R. L., "Don't Suppress the Wiggles - They're Telling You Something," Proc. Symposium on Finite Element Methods for Convection Dominated Flows, ASME Winter Annual Meeting, New York, Dec. 3-7, 1979.

15. Chung, T. J., Karr, G. R., and Miller, D. W., "Accuracy and Stability of Least Square Finite Elements in Fluid Mechanics," Invited paper, 16th Society of Engineering Science Meeting, Northwestern University, Sept. 3-6, 1979.

16. Karr, G. R. and Chung, T. J., "Optimal Control Penalty Least-Square Finite Elements in Convective Heat Transfer," Proc. National Conference on Numerical Methods in Heat Transfer, University of Maryland, Sept. 24-26, 1979.

17. Chung, T. J. and Karr, G. R., "Significance of Convective Term in Transport Equation," Proc. Symposium on Finite Element Methods for Convection Dominated Flows," ASME Winter Annual Meeting, New York, Dec. 3-7, 1979.

18. Bateman, H. (1929): "Notes on a Differential Equation Which Occurs in the Two-Dimensional Motion of a Compressible Fluid and the Associated Variational Problems," Proc. Roy. Soc. (London), Ser. A. Vol. 125, No. 700, pp. 598-618.

19. Bateman, H. (1930): "Irrotational Motion of a Compressible Inviscid Fluid," Proc. National Acad. Sci. U.S.A., 16, pp. 816-825.

20. Herrivel, J. W. (1955): "The Derivation of the Equations of an Ideal Flow by Hamilton's Principle," Proc. Camb. Phil. Soc., 51, pp. 344-349.

21. Serrin, J. (1959): "Mathematical Principles of Classical Fluid Mechanics," Handbuch der Physik, Vol. 8, pp. 125-262.

22. Finlayson, B. A. (1972): "The Method of Weighted Residuals and Variational Principles, Academic Press, New York.

23. Norrie, D. H. and deVries, G.(1975): "Application of the Pseudo-Functional Finite Element Method to Nonlinear Problems in Finite Elements in Fluids," Vol. 2, Ed. Gallagher, John Wiley and Sons, New York.

24. Carey, G. F. (1975): "A Dual Perturbation Expansion and Variational Solution for Compressible Flows Using Finite Elements, Finite Elements in Fluids," Vol. 2, Eds Gallagher, Oden, Taylor, and Zienkiewicz John Wiley and Sons, pp. 159-177.

25. Tricomi, F. (1923): "Sulle equazion: lineari alle derivate Parzial" di secondo ordine, di tipo misto, Rendiconti, Atti dell Academia Nazionale deri Linceri, Series 5, 14, pp. 134-247.

26. Neumann, J. von, and Richtmyer, R. K. (1950): "A Method for the Numerical Calculation of Hydrodynamic Shock, J. appl. Phys., 21, p. 232. March.

27. Courant, R., Friedrichs, K. O., and Lewy, H. (1947): "The Partial Equations of Mathematical Physics, IBM J., 1967, p. 215. (Trans. of original paper in Math. Ann., 100, p. 32)

28. Lax, P. D. and Wendroff, B. (1960): "Systems of Conservation Laws," Comm. pure and appl. Math., 15, p. 363.

29. MacCormack, R. W. (1969): "The Effect of Viscosity in Hypervelocity Impact Cratering, AIAA 66-354, pp. 1-7.

30. Murman, E. M. and Cole, J. D. (1971):"Calculations of Plane Steady Transonic Flows, AIAA J., 9(1), pp. 114-121, Jan.

31. Jameson, A. (1975): "Transonic Potential Flow Calculations Using Conservation Form," AIAA Paper 75-000, June.

32. Wellford, L. C. and Oden, J. T. (1975): "Discontinuous Finite Element Approximations for the Analysis of Shock Waves in Nonlinear Elastic Solids," J. comp. Phys., 19, p. 179.

33. Chung, T. J. and Hooks, C. G. (1976): "Discontinuous Functions in Transonic Flow," AIAA Paper No. 76-329.

34. Brainerd, J. J. (1969): "Shock Wave Similarity, Recent Advances in Engineering Sciences, Ed. A. C. Eringen, 12, 4, pp. 173-193.

35. Chan, S. T. K., Brashears, M. R., and Young, V. Y. C. (1975): "Finite Element Analysis of Transonic Flow by the Method of Weighted Residuals," AIAA Paper No. 75-79.

36. Chan, S. T. K. and Brashears, M. R. (1975): "Finite Element Analysis of Unsteady Transonic Flow, AIAA Paper No. 75-875, June.

37. Glowinski, R., Periaux, J., and Pironneau, O. (1976): "Transonic Flow Simulation by the Finite Element Method via Optimal Control," Proc. 2nd Intl. Symp. Finite Element Methods in Flow Problems, ICCAD, Italy.

38. Wellford, L. C., Jr., and Hafez, M. M. (1976): "Finite Element Analysis of Linear Elliptic-Hyperbolic Systems Using a Local Parabolic Region," Proc. 2nd Intl. Symp. on Finite Element Methods in Flow Problems, ICCAD, Italy.

39. Ecer, A. and Akay, H. U. (1976): "Application of Finite Element Method to the Solution of Transonic Flow, Proc. 2nd Intl. Symposium on Finite Element Methods in Flow Problems, Italy, June.

40. Klunker, E. B. (1971): "Contribution to Methods for Calculating the Flow about Thin Lifting Wings at Transonic Speeds - Analytical Expressions for the Far Field," NASA Technical Notes, NASA TN D-6530.

41. Landahl, M. T. (1961): "Unsteady Transonic Flow, Pergamon Press, New York.

42. Spring, D. J. (1973): "Comparisons Between Experiment and an Approximate Transonic Calculative Method," Tech. Report RD-73-36, U.S. Army Missile Command, Huntsville, Ala.

43. Trangenstein, J. A., "A Finite Element Method for the Tricomi Problem in the Elliptic Region," Ph.D. Thesis, Cornell University, 1975.

44. Aziz, A. K. and Levanthal, S. H., "Numerical Solution of Linear Partial Differential Equations of Elliptic-Hyperbolic Type," SYNSPADE 1975, Numerical Solution of Partial Differential Equations-III, Ed., B. Hubbard, Academic Press, Inc., 1976.

45. Friedrichs, K. O., "Symmetric Positive Linear Differential Equations," Comm. Pure Appl. Math., 11, 1958, 333-418.

46. LeSaint, P., "Finite Element Methods for Symmetric Hyperbolic Equations," Numer. Math. 21, 1973, 244-255.

47. Fix, G. J., and Gunzburger, M. D., "On Least Squares Approximations to Indefinite Problems of the Mixed Type," Int. J. Numer. Meth. Engineering, Vol. 12, 1978, 453-469.

48. Chung, T. J., "Convergence and Stability of Nonlinear Finite Element Equations, AIAA J., 13, No. 7, 1975, pp. 963-966.

49. Chung, T. J. and Chiou, J. N., "Analysis of Unsteady Compressible Boundary Layer Flow Via Finite Elements",Int. J. for Computers and Fluids, 4, No. 1A, 1976, pp. 1-12.